Earth's Future

RESEARCH ARTICLE
10.1029/2023EF004074

Observational Evidence Reveals Compound Humid Heat Stress-Extreme Rainfall Hotspots in India

Poulomi Ganguli[1] and **Bruno Merz**[2,3]

[1]Agricultural and Food Engineering Department, Indian Institute of Technology Kharagpur, Kharagpur, India, [2]GFZ German Research Centre for Geosciences Potsdam, Potsdam, Germany, [3]Institute of Environmental Sciences and Geography, University of Potsdam, Potsdam, Germany

Key Points:

- We quantify the exceedance probability of sub-daily rainfall peaks conditioned on preceding heatwaves
- A significant upward trend in the frequency of compound heatwave-extreme precipitation events is detected across all seasons
- Sub-daily rainfall peaks shows notable changes in their exceedance probability in response to changing heatwave properties

Supporting Information:

Supporting Information may be found in the online version of this article.

Correspondence to:

P. Ganguli,
pganguli@agfe.iitkgp.ac.in

Citation:

Ganguli, P., & Merz, B. (2024). Observational evidence reveals compound humid heat stress-extreme rainfall hotspots in India. *Earth's Future*, *12*, e2023EF004074. https://doi.org/10.1029/2023EF004074

Received 23 AUG 2023
Accepted 20 JAN 2024

Author Contributions:

Conceptualization: Poulomi Ganguli, Bruno Merz
Data curation: Poulomi Ganguli
Formal analysis: Poulomi Ganguli
Funding acquisition: Poulomi Ganguli, Bruno Merz
Investigation: Poulomi Ganguli
Methodology: Poulomi Ganguli, Bruno Merz
Project administration: Poulomi Ganguli
Resources: Poulomi Ganguli
Software: Poulomi Ganguli
Supervision: Bruno Merz
Validation: Poulomi Ganguli
Visualization: Poulomi Ganguli

Abstract Sequential climate hazards, such as "warm and wet" compound extremes, have direct societal implications for highly urbanized regions and agricultural production. While typically extreme temperatures and rainfall are inversely correlated during the summer, extreme humid heatwaves often lead to atmospheric instability and moisture convection, increasing the likelihood of extreme precipitation (EP). Little is known about how heatwave characteristics, such as peak intensity and duration, influence EP at a regional scale. Using high-resolution, sub-daily station-based observational records over five decades (1971–2021) across India, we find a robust increase in the frequency of compound humid heat-peak precipitation events in all seasons. Our sensitivity analysis of the impact of humid heatwave characteristics on the subsequent sub-daily rainfall extremes reveals that, with an increase in peak heatwave intensity for a given heatwave duration, >50% of sites show an increase in the magnitude of rainfall; conversely, with an increase in heatwave duration for a given peak heatwave intensity, around 67% sites show a decline in sub-daily rainfall extremes. An asymmetrical shift toward above-average precipitation extremes in response to humid heat stress is mainly clustered around low-elevation, densely populated coastal areas and the irrigation-intensive Indo-Gangetic Plains.

Plain Language Summary Compound humid heatwave-extreme rainfall events substantially impact society, as the sequential occurrence of such events has immense damage potential due to the limited recovery time compared to the situation where these events occur in isolation. Detecting spatiotemporal patterns in compound hot-wet weather extremes is essential for disaster management, projecting future changes, and devising an early warning system for vulnerable populations. Using gauge-based observations of more than five decades across India, we find a robust increase in the number of compound humid heatwave-extreme precipitation events over climatologically homogeneous regions of India across all seasons. We analyze how the rainfall extremes depend on the characteristics of the preceding heatwave: we find that rainfall extremes increase with increasing heatwave intensity for more than 50% of sites; in contrast, rainfall extremes decrease with increasing heatwave duration for around 67% of sites. A shift toward higher rainfall in response to humid heat characteristics is apparent in densely populated coastal areas and irrigation-dominated regions of the country.

1. Introduction

Extreme heat events in a warming environment have direct societal impacts affecting large populations within a short span, triggering health emergencies, loss of labor productivity and often excess mortality (WMO, 2023). Extreme heatwaves have caused over 25,000 fatalities in the Indian subcontinent between 1992 and 2020 (EM-DAT, 2023; Hindustan Times, 2022). The Indian subcontinent is emerging as a "hotspot" of extreme heatwave owing to global warming (Lenton et al., 2023; Tuholske et al., 2021). During 2022, record-breaking high temperatures and below-average rainfall from mid-March to April over northwestern parts of the country have adversely affected "Rabi" wheat crops before their harvest (FAO, 2022). This unprecedented increase in temperature in mid-March 2022 resulted in a 10%–15% decline in wheat production across major wheat growing areas, especially for late-planted wheat (Beillard & Singh, 2022). Further, several Indian regions have witnessed two contrasting yet consecutive extreme weather events, humid heatwave followed by extreme precipitation (EP), impacting human health (Bansal et al., 2023), forest and agriculture (You et al., 2023), infrastructure (Kotz et al., 2022; Prein et al., 2017) and energy demand (Stone et al., 2021). For instance, severe heatwaves in late May 1998 over the Indian subcontinent resulted in more than 2,500 fatalities, equivalent to a departure from the mean annual mortality of more than 3 times the standard

Writing – original draft: Poulomi Ganguli
Writing – review & editing: Bruno Merz

deviation (Figure 1). Within 2 weeks, these heatwaves were followed by tropical cyclone-induced unprecedented storms, impacting 4.6 Million people with estimated damage of over 0.8 billion USD (EM-DAT, 2023).

Studies showed an upward trend in heatwaves and an increase in spatial extents of hot-dry compound events in India (Guntu et al., 2023; Rajeev et al., 2022; S. Sharma & Mujumdar, 2017) and globally (Yin et al., 2022). Most of these assessments centered around hot-dry compound events with specific emphasis on "dry-bulb" temperature, or air temperature. However, high humidity precludes heat evacuation by evaporation, leading to humidity playing a critical role in escalating heat stress (Davis et al., 2016). In addition, higher surface temperatures and increasing downwelling infrared radiation due to anthropogenic climate change enhances surface evaporation, which increases the atmospheric moisture content and leads to extreme rainfall (Roderick et al., 2019; Trenberth, 1999). There is growing evidence of heavy rainfall following humid heatwaves both locally (Feng et al., 2022; Rajeev & Mishra, 2022; S. S.-Y. Wang et al., 2019) and worldwide (Sauter et al., 2023; Yin et al., 2022).

Figure 2 presents possible physical mechanisms driving Compound Moist Heatwave-Extreme Precipitation (CMHP) events over the Indian landmass. The elevated air temperature during heatwave episodes increases the moisture-holding capacity of the atmosphere, dictated by the Clausius-Clapeyron relation (Domeisen et al., 2022). Heatwaves associated with high humidity and temperatures can increase the precipitable water in the lower troposphere, which serves as a source of moisture. The risk of EP and flooding is enhanced by the joint evolution of high temperatures and humidity, which causes atmospheric instability and high levels of moisture convection (C. Li et al., 2023; W. Zhang & Villarini, 2020). Using reanalysis records, Y. Zhang and Boos (2021) demonstrated that extreme wet-bulb temperature, T_w, a multivariate metric considering temperature and humidity, is associated with an anomalously warm lower troposphere and high convective inhibition (CIN), which suppresses precipitation on the day before the annual maximum wet-bulb temperature for latitudes between 50°N and 50°S. In contrast, following the day of annual maximum T_w, cooling of the lower troposphere reduces CIN and enhances precipitation by around 70% compared to at-site summer rainfall (See Figure 2; Y. Zhang & Boos, 2021). However, this finding has to be treated with caution, as humid heatwaves often have a limited spatial extent and short duration, and are thus significantly underrepresented in reanalysis-based data sets over the monsoon-dominated regions of the tropics (Raymond et al., 2020). Further, their study suggested that the humid heat extremes are most frequent around the date of the regional southwest monsoon-induced rainfall onset. Using gridded observational records, Robinson et al. (2021; see their Figure 2) have found that the tropics, for example, peninsular India, showed the most pronounced upward trends in heat and wet extremes. However, this study evaluated the decadal changes in heat and rainfall extremes separately, without accounting for the joint evolution of both hazards. At a local scale, recent studies have shown that urbanization intensifies not only humid heatwaves owing to the "Urban Heat Island" effect (UHI; Figure 2; Ortiz et al., 2018; J. Yang et al., 2023; K. Zhang et al., 2023), but also affects local weather patterns, such as enhancement of mean rainfall and short-duration extreme rainfall by increasing vertical uplift and moisture convergence (Ali et al., 2021; Fischer & Knutti, 2016; Y. Li et al., 2020; Liu & Niyogi, 2019; Vo et al., 2023). This amplifies the likelihood of "preconditioned" compound extremes, that is, the sequential occurrence of humid heatwaves and extreme rainfall (C. Li et al., 2023; W. Zhang & Villarini, 2020; Zscheischler et al., 2020).

Heatwaves in India result mainly from the advection of heat from neighboring regions, and from smaller contributions of local heat fluxes (Nageswararao et al., 2020; Singh & Kumar, 2018). In India, three types of heatwaves were identified (Ratnam et al., 2016; Wehner et al., 2016; Guo et al., 2022; Figure 2): (a) Unusual atmospheric "blocking" over the North Atlantic Ocean frequently coincides with the heatwaves that affect northern and central India. A cyclonic anomaly develops at upper levels west of Northern Africa due to blocking over the North Atlantic Ocean. The warming sea surface temperature (SST) of the North Atlantic Ocean can trigger quasistationary Rossby waves over Eurasia (X. Yang et al., 2021). A larger number of hot days in northwestern and north-central India result from these quasistationary Rossby wave trains and an "upper-level cyclonic anomaly" over western North Africa (Qin et al., 2023; Ratnam et al., 2016; Satyanarayana & Rao, 2020). The northwestern region experiences elevated humid heatwaves during July-August, associated with anomalous positive specific humidity and negative outgoing long radiation anomalies (Ivanovich et al., 2022). In contrast, (b) heatwaves over the eastern coastal region, that is, the part of central northeast and peninsular India (Figure S1 in Supporting Information S1), are associated with westerly wind anomalies, which lessen the land-sea wind along the coastal region (Wehner et al., 2016). Due to low soil moisture and clear skies, this region experiences heatwaves from March through May because of the prolonged advection of strong "hot and dry" wind (referred to

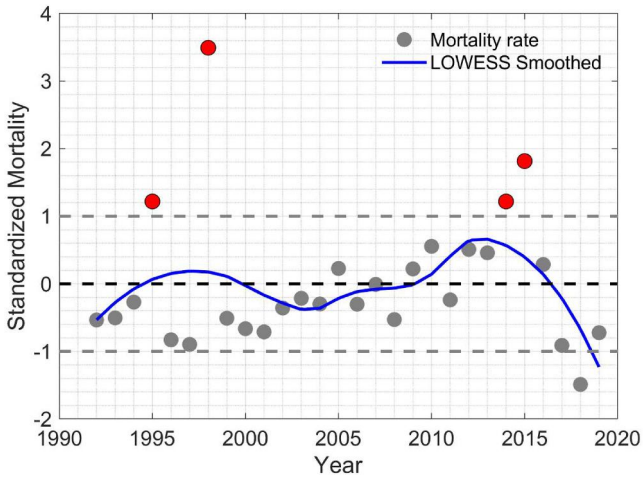

Figure 1. Observed annual mortality rate related to heat stress in India for 1992–2019 based on GSDMA (2023). The standardized mortality is shows the magnitude of anomaly from the long-term annual mean and determined for each year as the deviation from the mean annual series ($M - \overline{M}$, where $\overline{M}$ is the annual average mortality) to the standard deviation of the annual mortality time series. The solid line in blue shows the standardized anomaly series smoothed using the LOWESS fits. Years with positive anomalies greater than one standard deviation are shown using red filled circles.

as "Loo" in the Indian subcontinent) from Pakistan across northwest India (Nageswararao et al., 2020). However, humid heatwaves in this region develop during the monsoon break period, that is, dry short-duration spells during June-September. The circulation anomalies associated with the short-term climate modes Madden-Julian Oscillation and Boreal summer intra-seasonal oscillation may be responsible for the "break spell" followed by elevated humid heatwave intensities during May through June over south-eastern India (Ivanovich et al., 2022). (c) Over the Indo-Gangetic Plains (IGP), the region that spans vast stretches from Jammu and Kashmir in the western Himalayan range to the lower Ganges Delta including the north-eastern Indian State of Assam, humid heatwave tends to be more severe in the pre-monsoon (April-May) and post-monsoon (October-November) seasons than in the monsoon (June-September) season owing to the massive extents of irrigated areas (Guo et al., 2022).

Atmospheric circulation patterns and anomalies in soil moisture are crucial factors in developing heat extremes (Wehrli et al., 2022). In the tropics, especially in regions with a dominant monsoon season, the effects of soil moisture are particularly important. Large-scale daytime advection dries up already-desiccated soil, creating a positive feedback loop between heatwave and soil drying (Figure 2; Miralles et al., 2019; Perkins, 2015). Increased boundary layer growth due to reduced soil moisture leads to "heat entrainment," enabling heat build-up in the vertical profile of the atmosphere (Perkins, 2015).

While observational and modeling evidence suggests an increase in surface specific humidity in response to global warming, the nonlinear relation between sub-daily precipitation extremes and moist heatwave characteristics, such as duration and peak intensity, remains poorly understood (Domeisen et al., 2022; Willett

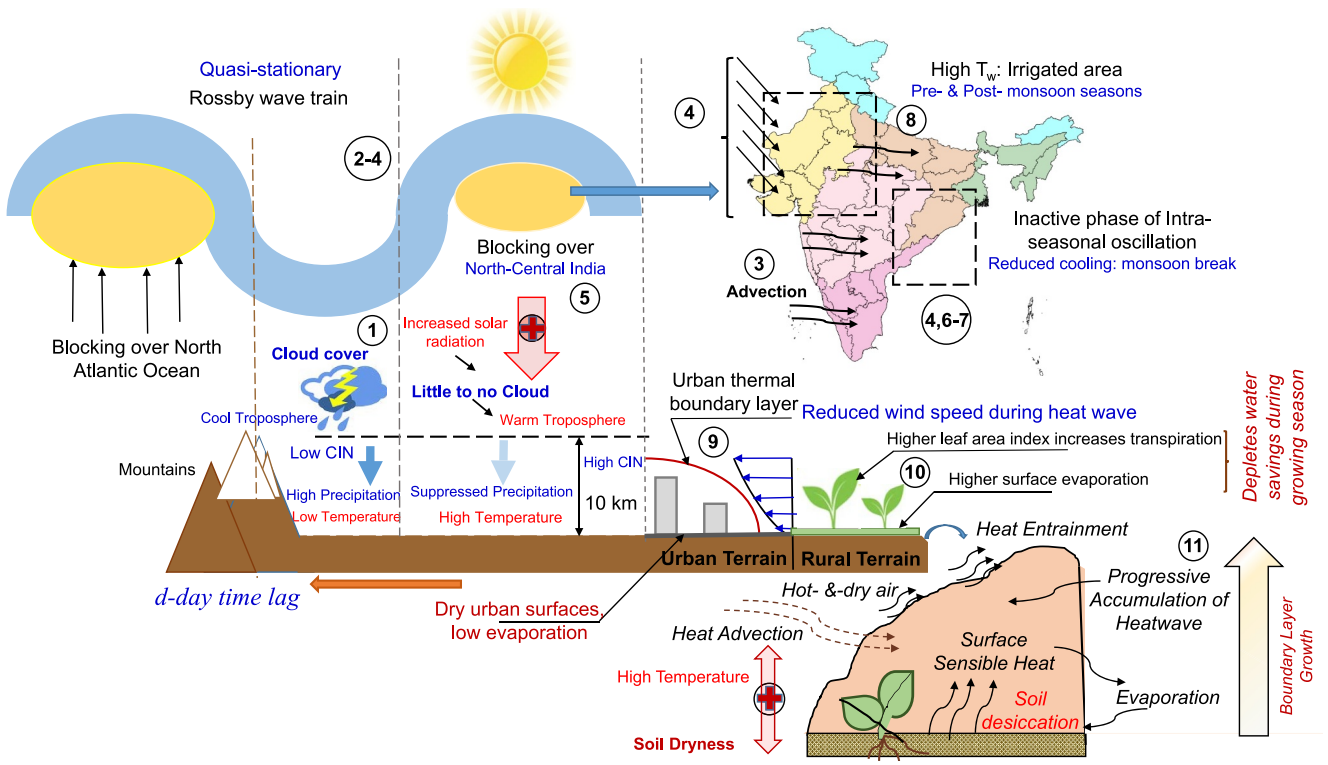

Figure 2. Summary of state-of-the-art knowledge of humid heat stress-extreme rainfall. The numbers corresponding to the citations are included in Table S1 in Supporting Information S1.

et al., 2007). Ye et al. (2016) demonstrated that rising air temperatures in northern Eurasia coincided with increased precipitation intensity but decreased frequency. In a companion paper, Ye & Fetzer (2019) evaluated the changing patterns of summer dry spell lengths across 517 Russian stations over 45 years (1966–2010). They detected that a hot summer favors more frequent and longer-lasting dry spells, triggering heatwaves and droughts when the air temperature is high. These studies were purely based on mean daily dry-bulb temperature and did not consider heatwave peaks. Second, they have neither considered the concurrence of humid heatwaves and precipitation extremes nor the lag time between these two variables, a determinant of compound hazard. However, analyzing the sequential occurrence of humid heatwaves and rainfall extremes is crucial because their joint impact may be particularly severe as the affected region may not have been recovered from the first event when the second event hits.

Although some studies have investigated CMHP events using bivariate probabilistic models, none has offered an approach to quantify EP probability conditioned on preceding heatwaves characteristics. However, this information is crucial for assessing the joint impact of CMHP hazards and to inform stakeholders, such as the insurance sector (Hino & Burke, 2021; Kruczkiewicz et al., 2021). Further, most concurrent hazard assessment research concentrated on mid-latitude to sub-tropical locations (Bui et al., 2019; Fowler et al., 2021; C. Li et al., 2023; Ning et al., 2022; You & Wang, 2021; W. Zhang & Villarini, 2020). In contrast, very few have investigated the tropical region or developing nations with the least capacity to adapt to back-to-back compound climatic hazards resulting from heat stress and extreme rain events (Im et al., 2017). Leveraging ground-truth observations of around five decades, we introduce a novel probabilistic approach that quantifies, for the first time, expected precipitation exceedances conditioned on the key characteristics of the preceding heatwaves, using a copula-based conditional joint probability method (Nelsen, 2013).

2. Material and Methods

2.1. Hydrometric Observations

We retrieved at-site hydrometric observations from 30 urban and peri-urban locations across India from the IMD's Data Supply Portal, (https://dsp.imdpune.gov.in/data_supply_service.php#procedure) at a sub-daily timescale of 3-hourly intervals for 1970–2021 sampled between 8:30 a.m. and 5:30 p.m. Indian standard time (3:00 to 12:00 hr UTC). These sites were selected based on data completeness and availability of meteorological records. We eliminated three stations which failed to pass the detailed quality-control procedures of Raymond et al. (2020). The selected 27 stations are distributed over six homogeneous monsoon sub-regions of India (Maharana & Dimri, 2014; Table S2 and Figure S1 in Supporting Information S1).

To assess the physical drivers of CMHP events, we analyze the roles of atmospheric moisture transport during the 40-year climatology from 1979 to 2018. First, we determine the vertically integrated moisture transport (VIMT; Lélé et al., 2015) from the composite of zonal and meridional components of moisture flux obtained from ERA-Interim, the third generation reanalysis product of the European Centre for Medium-Range Weather Forecasts (ECMWF) at a 0.75° grid resolution (van Zomeren & van Delden, 2007). Next, we determine changes in the VIMT composite for the monsoon months and the entire year. We use ERA-Interim instead of the newer reanalysis versions, such as ERA5, for the following reasons: (a) ERA5 consistently underestimates the southwest monsoon signal in the late monsoon season to early winter (until December) compared to ERA-Interim (Hassler & Lauer, 2021). (b) Over the Himalayan regions, ERA-Interim outperforms ERA5 (Nogueira, 2020).

2.2. CMHP Event Identification

A humid heatwave event is detected when the daily maximum wet-bulb temperature from 3-hourly observations exceeds a pre-defined threshold persistently for at least 4 days (Ceccherini et al., 2017). The threshold is set to the 90th percentile of the daily maximum wet-bulb temperature using a 31-day rolling window over a calendar year (Figure S2 in Supporting Information S1). Therefore, the threshold varies throughout the year, and heatwaves are detected in all seasons (Ceccherini et al., 2017). While the public is more aware of summer heatwaves, which have substantial health impacts on human and livestock, winter heatwaves or warm spells impact crops, shorten the duration and rate of grain filling, accelerate desiccation of plants, and cause early senescence, especially for wheat (Leach et al., 2021; Lobell et al., 2012; Loughran et al., 2017). Second, several regions in India experience heatwaves during late winter (February-March) and early spring, increasing the risk of forest fires (Chauhan, 2023; IMD, 2022; Mohan, 2023). Third, extreme heatwaves have triggered pre-monsoon rainfall during

March-May and thunderstorms across several parts of India, resulting in crop damage and flash floods (Bose, 2023).

We characterize heatwave events using peak intensity (i.e., amplitude), duration and the mean timing of the peak intensity of a humid heatwave event (Domeisen et al., 2022). The peak intensity refers to the warmest day of the heatwave episode, duration indicates its total spell length from the date of initiation to its termination (See Figure S2 in Supporting Information S1). While heatwave peak intensity is a crucial metric for assessing labor productivity, human health, and infrastructure resilience (Keellings & Moradkhani, 2020), the spell length is crucial for assessing its impact on sequential weather and climate hazards, such as dry/wet spells (Mukherjee et al., 2023; You & Wang, 2021).

The rainfall measurement is available at a 3-hourly interval. EP is the sub-daily maximum rainfall above the predefined rain threshold, where the rain threshold is fixed as the 50th percentile of the sub-daily rainfall throughout the analysis period. CMHPs are defined for two cases. First (Case I), they are detected when the peak intensity of a humid heatwave event T_w, that persists for >3 consecutive days, precedes the EP in a time window of $t \, \epsilon \, [-1, 7]$. A time window of 1 week captures lag times commonly used in the literature (Ilampooranan et al., 2019; Kemter et al., 2020). A lagged response between heatwaves and EP may stem from atmospheric circulation, shifts in the synoptic environment, and land-sea atmospheric feedbacks (Raghavendra et al., 2019; W. Zhang & Villarini, 2020). Further, a slow-moving tropical cyclone, accompanied by a storm, often follows a heatwave due to changes in atmospheric circulation (Feng et al., 2022; Matthews et al., 2019; Simpkins, 2023; P. Wang et al., 2023). As a second case (Case II), we consider CMHP events when the annual maximum wet-bulb temperature ($T_{W\max}$) precedes the EP during the specified time window. Since annual maxima events are sampled once per year, duration is not considered in Case II. To ensure two successive CMHP events are independent in Case I, we maintain a minimum separation period of 3 days between the heatwave intensity peaks (Barton et al., 2016). The time window of $[-1, 7]$ also allows situations where the extreme rainfall occurs at the same day of the heatwave peak or one day prior to the peak. This choice is meant to consider those situations where the EP occurs during the initial development phase of the heatwave. The assessment of negative and positive lag time proportions (Figure S3 in Supporting Information S1) shows positive lagged responses for ≥80% of compound occurrences for both cases, confirming that heatwaves precede EP for most sequential occurrences.

At first, we statistically demonstrate a link between preceding humid heatwaves and the following EP events. For this, we sample EP events with and without preceding humid heatwaves for different seasons and for the whole year. Then, we compare the distributions and the tail behavior of EP for the two conditions (with/without preceding heatwave). We identify locations prone to CMHP events based on the following event-specific attributes: (a) Strength of dependence of humid heatwave peak intensity (T_w, $T_{w\max}$) and EP magnitude using the scale-free correlation metrics Kendall's τ (measuring complete dependence) and the upper-tail dependence coefficient λ_U (AghaKouchak et al., 2013; Serinaldi et al., 2015). (b) Response time or lag time between humid heatwave intensity peak (T_w, $T_{w\max}$) and the following EP. (c) For Case I, annual frequency (number) of CMHP events for each site. The response time (Gori et al., 2020; Lyddon et al., 2023) is a crucial factor contributing to the hazard potential of compound extremes. A short response time between CMHP drivers indicates that peak humid heatwave amplitude and peak rainfall occur in swift succession, leaving less time for recovery and leading to more extreme impacts. In contrast, a longer response time indicates a lower likelihood of the co-occurrence of two peaks.

The seasonal frequency (i.e., counts) of CMHP occurrences for each year is then determined to comprehend the seasonal variations of CMHP events and their temporal evolution over the period 1971–2021. For each season (pre-monsoon: March-May, monsoon: June-September, post-monsoon: October-December, winter: January-February), we count the number of CMHP occurrences in each year obtained from Case I. Those events are excluded in the seasonal analyses where the heatwave peak occurs at the end of a season, and the rainfall occurs in the next season. Then we implement an 8-year moving average to assess the decadal to inter-annual variability in CMHP extremes. To shed light on the drivers of CMHP events, we compare the spatial patterns of composite anomalies (monsoon season—all seasons) of daily-averaged VIMT on the day of peak intensity T_w (or annual maxima $T_{w\max}$) versus the precipitation days following the heatwaves. The VIMT anomalies during monsoon versus all seasons help to understand whether the generated moisture transport results from convection-induced moisture instability or large-scale monsoon-induced moisture transport, because wind convergence and water vapor advection play a crucial role in moisture convergence (extreme rainfall) or divergence (dry spells) during the monsoon season (Held & Soden, 2006; Rajeevan et al., 2008).

2.3. Trivariate Copula-Based Conditional Joint Probability Framework

We use a trivariate copula function (Nelsen, 2013) to determine joint probability distributions of EP and heatwave characteristics, that is, peak intensity and duration. Copula functions join d-dimensional independent marginal distributions based on their dependence structures. The nature of dependency of pair-wise CMHP drivers is assessed using complete and upper tail (low-probability/high-impact events) dependency estimators (Capéraà-Fougères-Genest; Frahm et al., 2005). We apply Kendall's τ to quantify the complete strength of dependence, that is, degree dependence considering pair-wise values of two variables, and the (upper) tail dependence coefficients λ_U (Serinaldi et al., 2015; Text S1.1 in Supporting Information S1) to quantify the joint occurrence of the two extreme events. While Kendall's τ encapsulates the likelihood that one variable exceeds its median given that the other variable exceeds its median, the upper tail dependence coefficient describes the correlation between the upper parts of two or multiple random variables. For a bivariate distribution, the upper-tail dependence indicates the probability that one variable exceeds a high threshold value (in the rank-transformed data) given that the other variable has already exceeded the same threshold (AghaKouchak et al., 2013).

The conditional probability of EPs exceeding a certain threshold ($\boldsymbol{R} > r$) conditioned on the T-year event peak heatwave intensity ($I = i$) and n-day event duration ($D = d$) is expressed as (L. Zhang & Singh, 2019)

$$f_{\boldsymbol{R}|I,D} = \frac{f(r,i,d)}{f(i,d)} = c_{\boldsymbol{R},I,D}\left[F_I(i),F_D(d),F_{\boldsymbol{R}}(r)\right] f_I(i) f_D(d) \tag{1}$$

$c_{\boldsymbol{R},I,D}(\cdot)$ in Equation 1 indicates copula-based joint probability density function of CDF, $\boldsymbol{C}_{\boldsymbol{R},I,D}[F_I(i),F_D(d),F_{\boldsymbol{R}}(r)]$. $f_I(i)$ and $f_D(d)$ are the PDFs of the marginal distributions of peak heatwave intensity and corresponding heatwave event duration. Finally, the conditional exceedance probability of EP events (i.e., $\overline{F}_{\boldsymbol{R}|I,D}(\boldsymbol{R} > r|I = i, D = d)$ can be obtained using the concept of cumulative exceedance probability (or complementary CDF, CCDF), $f_{\boldsymbol{R}|I,D}$ for $\boldsymbol{R} > r$, which is expressed as (Refer page 118 in L. Zhang & Singh, 2019)

$$\begin{aligned}\overline{F}_{\boldsymbol{R}|I,D}(\boldsymbol{R} > r|\, I \le i, D \le d) &= \int_r^{\infty} f_{\boldsymbol{R}|I,D}(u|\, i,d)\, du = 1 - \int_0^{\boldsymbol{R}} f_{\boldsymbol{R}|I,D}(u|\, i,d)\, du \\ &= 1 - F_{\boldsymbol{R}|I,D}(\boldsymbol{R} \le r|\, I = i, D = d) \\ &= 1 - \frac{\boldsymbol{C}_{\boldsymbol{R},I,D}\left[F_I(i),F_D(d),F_{\boldsymbol{R}}(r)\right]}{\boldsymbol{C}_{I,D}\left[F_I(i),F_D(d)\right]}\end{aligned} \tag{2}$$

where $\boldsymbol{C}_{I,D}[F_I(i),F_D(d)]$ is the copula-based bivariate joint CDF of peak heatwave intensity and duration. $F_I(i)$, $F_D(d)$ and $F_{\boldsymbol{R}}(r)$ are the marginal CDFs of peak intensity, heatwave duration and sub-daily EP magnitude. We use the metaelliptical Student's t copula to model the trivariate joint distribution, which enables fitting the upper tail dependency satisfactorily. Following Genest et al. (1995), we determine the parameters of the selected copula using the maximum pseudo-likelihood method. The best-fitted copula models are assessed based on the standard goodness-of-fit procedure, that is, the bootstrap-based Cramer von Mises distance statistic, which is the summation of the squared distance of empirical versus fitted continuous distribution functions (Genest et al., 2009; Text S1.2 and Table S3 in Supporting Information S1). The graphical comparison between empirical and Student's t copula family (Figure S4 in Supporting Information S1) indicates that Student's t copulas perform well in modeling the joint probability and the upper tail dependencies between driver pairs.

Ties, that is, repeated values, can influence the fitting performance of probability distributions. Duration and EP series often contain repeated values. Therefore, we use a physically informed approach (Moccia et al., 2021; Salvadori et al., 2014) to handle ties by adding random noise with a range of 0.001 to 0.0001 to each data point in the series. This results in a "statistically equivalent value" so that each sample has a distinct rank without changing the distributional properties of the observed series. Further, we evaluate trends in each CMHP driver employing the Mann-Kendall test for monotonic trends with a correction for repeated observations and autocorrelation at a 5% significance level (M. J. Reddy & Ganguli, 2013; Tables S4 and S5 in Supporting Information S1). Next, we evaluate the trend slope using the Theil-Sen regression (Sen, 1968), in which the slope is computed as the median slope of all possible data points pairs. For series with a significant trend in peak heatwave intensity and sub-daily EP, we model the marginal distributions using the nonstationary generalized extreme value (GEV) distribution

(see Text S1.3 in Supporting Information S1; De Leo et al., 2021). Since heatwave duration does not show significant trends, following an earlier assessment (Mazdiyasni et al., 2019), marginal distributions of heatwave duration are modeled considering several options: Log-logistic, Gamma, GEV with stationary assumption, Log-normal, and Generalized Pareto distributions. We select the distribution from the fitted probability models with the minimum value of the Akaike Information Criterion corrected for small sample size (Burnham & Anderson, 2003). We assess the goodness-of-fit of the selected distribution following the Kolmogorov-Smirnov (KS) test at the 5% significance level (Tables S6–S8 and Figures S5–S7 in Supporting Information S1).

To evaluate the sensitivity of EPs to humid heatwave characteristics, using the trivariate copula function, we analyze the relative changes in exceedance probability of above-average EPs in two different scenarios: (a) for the 10-year humid heatwave peak intensity T_w and varying heatwave durations, $d = 6$, 7, 8, 9, and 10 days relative to 5-day events, (b) for the 5-day heatwave duration d and varying return periods (2, 5, 15, 20, 25, and 50-year) of heatwave peak intensities T_w relative to the 10-year event. The 10-year peak intensity T_w indicates a very extreme temperature that has an exceedance probability of 0.1 (Seneviratne et al., 2021), and 5- to 10-day heatwaves pose a substantial challenge for society.

3. Results

3.1. Observational Link Between Preceding Heatwaves and the Following Extreme Precipitation Events

To understand whether there is a link between heatwaves and subsequent extreme rainfall, we sampled sub-daily maximum rainfall magnitude, which is above 50th percentile rainfall throughout the analysis period, with and without preceding humid heatwaves for different seasons and for the whole year. We find that the distributions of sub-daily rainfall with and without preceding heat stress are statistically distinct as detected by the two-sample Kolmogorov-Smirnov (KS) test with a p-value <0.05. The density plots of rainfall magnitude show similar differences between the two situations (with/without preceding humid heat stress) with the exception of the pre-monsoon (March-May) season (Figure 3). For all seasons and the entire year, the mean rainfall intensity is higher for events without preceding heatwave. However, their tails decay faster, while the rain events preceded by humid heatwave episodes show a heavier tail with multiple peaks for larger magnitudes. A relatively low magnitude of rainfall in the pre-monsoon season could be a consequence of the limited moisture availability at higher temperatures during the summer months (Fowler et al., 2021). The higher variance and the heavier tail of rainfall preceded by humid heatwaves in all seasons except for the pre-monsoon season suggests differences between mean and more extreme sub-daily rainfall in response to preceding heat stress.

Following the literature (Ha et al., 2022), we characterize the heatwave events as dry and humid based on relative humidity below 33% and above 67%, respectively, to further decipher the influence of heatwave type on the intensity of extreme rainfall. When EPs are not preceded by heatwaves, they show the highest variability with a sample variance of >2 mm^2 and are accompanied by multiple peaks in the density functions (Figure 4). While in the pre-monsoon season, the density function between the extreme rain following dry and humid heatwaves is statistically indistinguishable with a p-value of 0.26, the PDF of EPs preceded by humid heatwave show a slight rightward shift, indicating a slightly increased magnitude of rain (Figure 4a). The median rain magnitude of EPs following dry and humid heatwaves versus the EPs without preceding heatwaves remains the same during the pre-monsoon season. This could be because of the high temperature and low relative humidity during the dry summer compared to the other seasons. During the monsoon season, the variability of EPs following dry heatwaves is the lowest, whereas the EPs following humid heatwaves show a highly skewed distribution with a large number of outlying events (Figure 4b). In all seasons, EPs following humid heatwaves show positively skewed distributions, indicating a shift towards the wetter part of the distribution (Figure 4a–4e). In contrast, EPs following dry heatwaves show negatively skewed distributions during monsoon and winter (Figures 4b and 4d), indicating a shift towards the dryer part of the distribution. We find the highest positive skewness during the monsoon season for EPs following humid heatwaves, which is approximately 10% higher than EPs without preceding heatwaves (Figure 4b). Considering the whole year, without seasonal partitions, the median EP values for the events following humid heatwaves show the highest value compared to the EP events that are preceded by dry and without heatwaves (Figure 4e). Further, except during the pre-monsoon season, EP events followed by humid versus dry heatwaves are statistically distinct, as confirmed by the two-sample KS test at a 5% significance level.

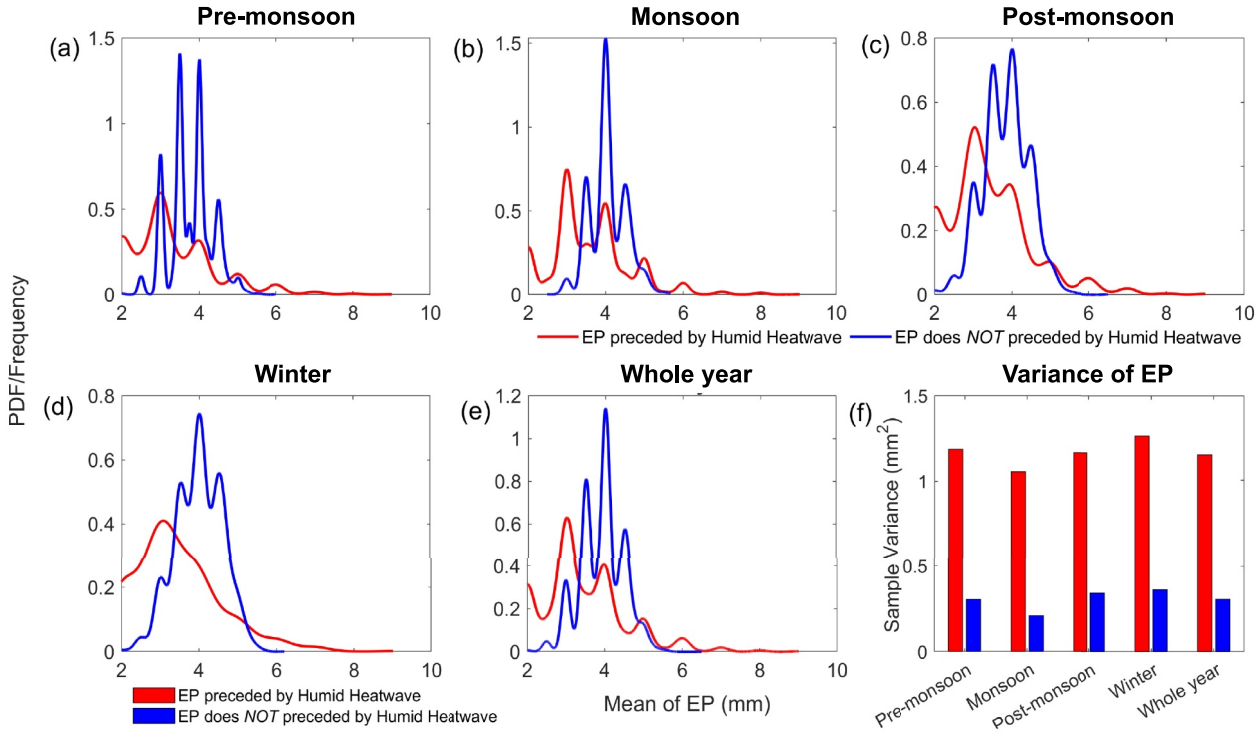

Figure 3. The distribution of sub-daily rainfall extremes, that is, extreme precipitations (EPs) with (in red)/without (in blue) preceding humid heatwaves. (a) Pre-monsoon (March-May), (b) Monsoon (June-September), (c) Post-monsoon (October-December), and (d) Winter (January-February) seasons, (e) Annually without seasonal partitions. The changes in the distribution of EPs with and without preceding heatwave are statistically significant, as confirmed by the two-sample Kolmogorov-Smirnov (KS) test. (f) Comparison of variance in EPs with versus without preceding heatwave. EPs preceded by heatwaves show larger variance in all cases as compared to those without preceding heatwaves. The two-sample *F*-test for the equality of variance shows statistically significant changes with a p-value < 0.05 for the EPs with and without heatwaves for all seasons and the entire year. If two or more sites reported extreme rainfall on the same day, then mean of the maximum sub-daily rainfall magnitude was considered.

3.2. Trends in Individual Drivers

The humid heatwave peak intensity (T_w) and the annual maxima ($T_{w\max}$) show a few significant but rather weak increases across the central-northeast, west-central and peninsular zones of India, whereas weak to negative changes are apparent over the central northeast and peninsular regions (Figures 5a and 5b; Table S4 in Supporting Information S1). Around 11% of the stations (3 out of 27), namely Nagpur and Hyderabad in the west-central region and Bhubaneshwar city in the central northeast region, show a statistically significant (at 5% significance level) trend in T_w (Table S4 in Supporting Information S1). The upward trends in T_w in these cities range from 0.13°C (Hyderabad) to 0.22°C (Bhubaneswar) decade^{-1}. In contrast, Gorakhpur in Central northeast and Coimbatore in peninsular India show a downward trend in T_w, ranging from −0.13°C to −0.2°C decade^{-1} (Table S4 in Supporting Information S1). Considering $T_{w\max}$, a higher number of stations (8 out of 27 or 30%) show statistically significant increasing trends (Table S5 and Figure 5b). Further, the statistically significant increasing trend in $T_{w\max}$ ranges from 0.27 (New Delhi) to 0.35°C (Thiruvananthapuram) decade^{-1} (Table S5 in Supporting Information S1). An increasing trend in $T_{w\max}$ over Thiruvananthapuram could be contributed to its proximity to the coast (Figure S8 in Supporting Information S1). Nagpur city in the west-central climatic region and Bhubaneshwar city located in the central-northeast region show statistically significant, increasing trends in both heatwave indicators T_w and $T_{w\max}$ (Tables S4 and S5 in Supporting Information S1). Among the stations with significant increasing trends in humid heatwaves, except a few cities, such as Thiruvananthapuram and Bhubaneswar, all cities belong to "urban agglomeration (UA)" cities (a city with multiple adjoining towns with a continuous outgrowth with a population of 1 million and above) as per the Census 2011 (ORGCC, 2022). Figure S8 in Supporting Information S1 portrays urban population versus trends in humid heatwaves as a function of distance to the sea. While the cities with less than 2 million population spread across the entire range of downward and upward trends, the UA cities with large population show primarily upward trends. Urbanization and industrialization potentially develop a "dome-shaped" temperature profile, and in the UAs, each city can develop

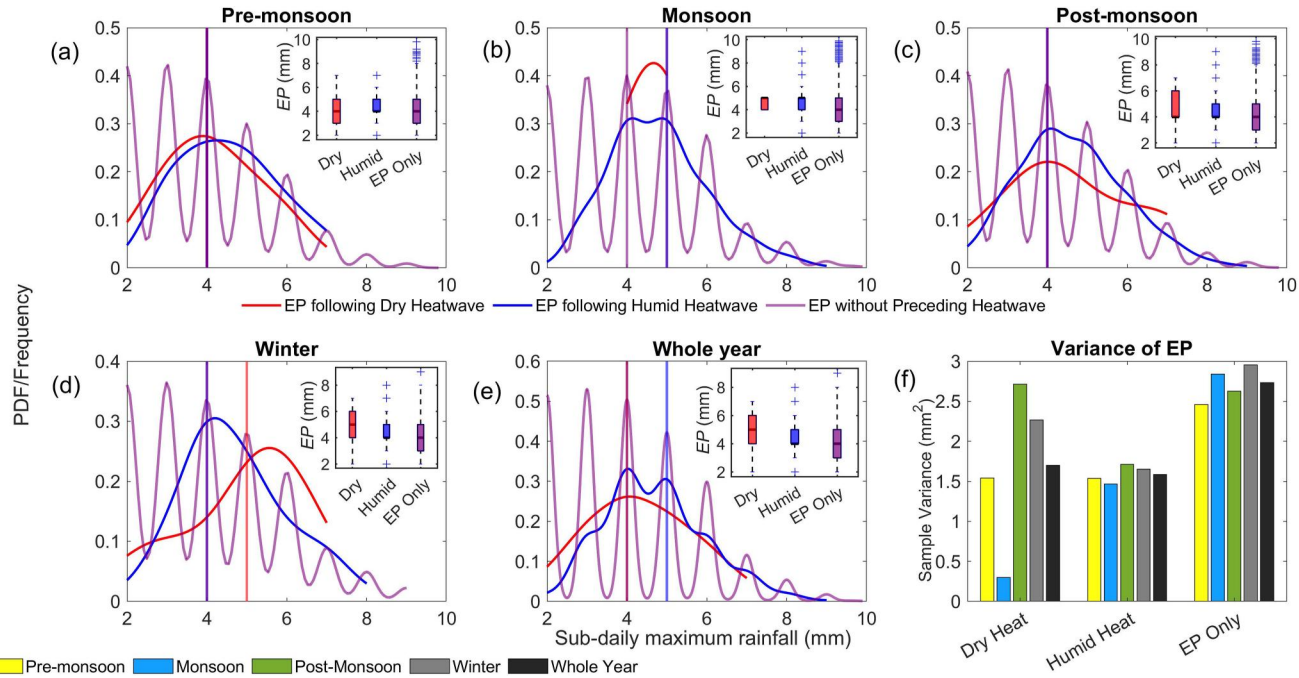

Figure 4. Density comparisons of extreme precipitations (EPs) preceded by dry (with relative humidity, i.e., Rh < 33%) and humid (Rh > 67%) heatwaves versus EP without preceded by heatwaves. The vertical lines in red, blue, and violet show the median marks of the EP events following the dry and humid heatwaves and the one without following heatwaves. The inset compares the boxplots of EPs for all three cases portraying their distinct quartiles, such that (i) Dry: EPs preceded by dry heatwaves (ii) Humid: EPs preceded by humid heatwaves (iii) EP Only: EP without preceded by heatwaves. The horizontal line marked in black within the box shows the median value. The median value for the EPs preceded by the humid heatwave events often coincide with its third quartile mark, suggesting a highly skewed distributions. The outlying events are shown in blue using "+" symbols.

a distinct heat dome escalating urban humid heatwaves (Fan et al., 2017; J. Yang et al., 2023; K. Zhang et al., 2023). Considering annual maxima T_{wmax}, a higher number of stations across southern India show significant trends as compared to northern India (Figures 5a and 5b). Heatwave duration does not show significant trends for any stations (Table S4 in Supporting Information S1).

The EPs following the heatwave events (Figures 5c and 5d; Tables S4 and S5 in Supporting Information S1) show mostly non-significant changes and some spatially confined decreasing trends. For Case I, 37% sites (10 out of 27) show a statistically significant decrease in EPs following peak intensity T_w. A decrease is observed over hilly, central-northeast, northeast, northwest, west-central, and peninsular India. Statistically significant downward trends in EP following T_w are observed over Prayagraj, Bhopal, Mumbai, and Coimbatore, ranging from −0.17 mm (Prayagraj) to −0.2 mm (Coimbatore) decade^{-1}. Akola City in West Central India shows the highest increasing trend in EP with a rate of 0.20 mm decade^{-1} (Table S4 in Supporting Information S1), however, the upward trend remains statistically insignificant. For Case II, a decrease in EPs following the annual maxima T_{wmax} is observed over 40% of the sites (11 out of 27), mainly clustered around northwest, west-central, and peninsular India, ranging from −0.30 mm (Nagpur) to −0.59 mm (Bengaluru) decade^{-1}(Table S5 in Supporting Information S1). EPs in Bhopal and Mumbai, located in the west-central region, show a decreasing trend in both cases. Although heatwave intensity has increased significantly across 11%–30% of the locations for T_w and T_{wmax}, the changes in subsequent EPs are small, although statistically significant. However, trend analyses show mean changes and do not necessarily reflect non-linear shifts or changes in rare events.

3.3. Mean Timing of Humid Heatwaves

The mean time of peak T_w intensity (and annual T_{wmax}) is mainly concentrated during the monsoon season, which contributes the largest share of heatwaves to 30%–59% of sites considering both cases I and II (Figures S9a and S9b in Supporting Information S1). The mean timing of humid heatwaves across the central northeast, particularly, the IGP and peninsular regions is concentrated around the pre-monsoon (February-May) season, which supports previous assessments that the increased T_w in the IGP during the pre-monsoon period is attributed to

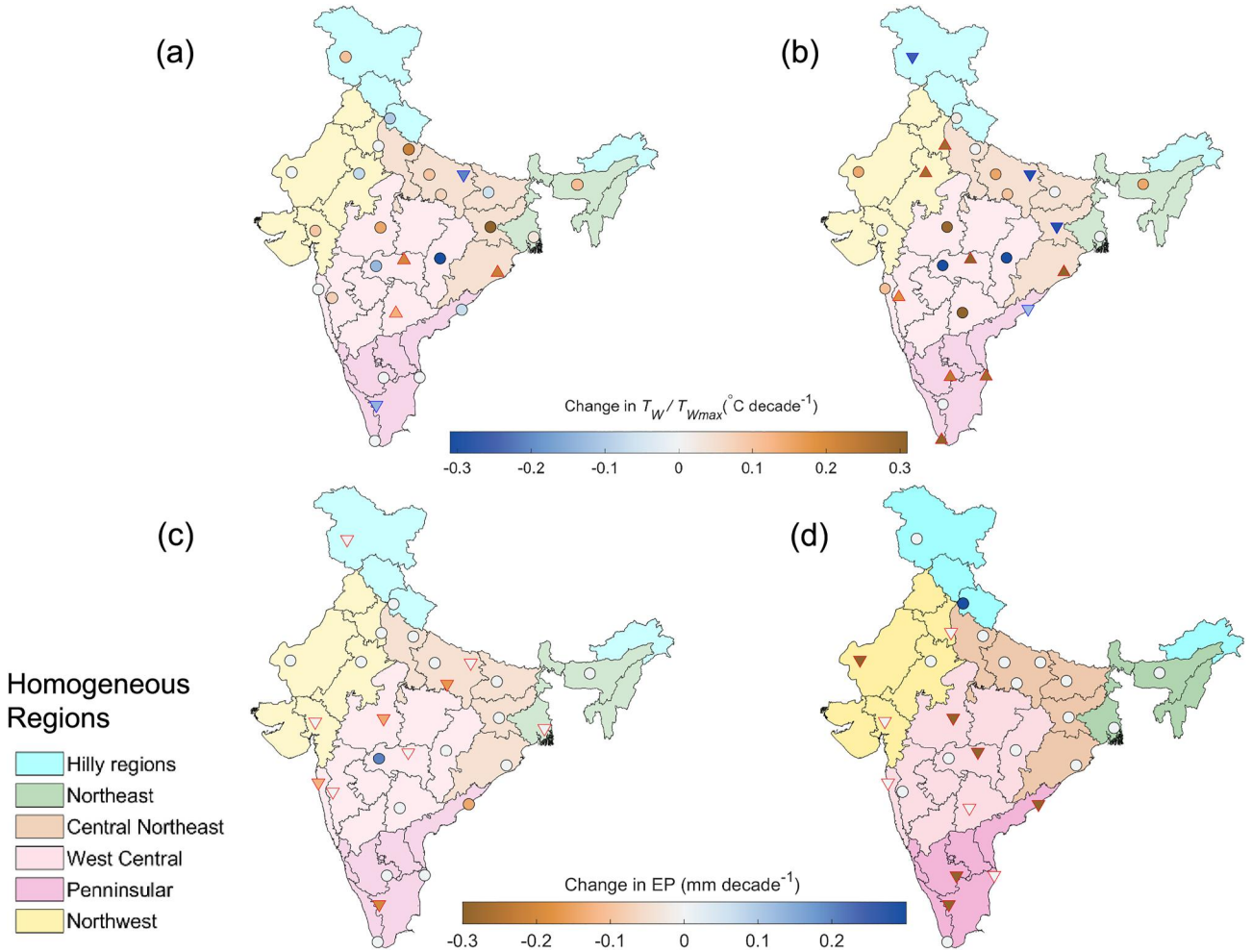

Figure 5. Trends in compound drivers: peak heatwave intensity T_w (a), annual maxima wet-bulb temperature $T_{w\max}$ (b), and the following sub-daily maximum rainfall (c, d). The top row shows the (a) Humid heatwave peak intensity T_w and (b) annual maximum of T_w events, while the bottom row shows the following extreme precipitation (EP) events correspond to (c) T_w and (d) $T_{w\max}$. A significant increase (decrease) is indicated using an upward (downward) triangle with $p < 0.05$ based on the nonparametric Mann-Kendall trend test. An increase in peak heatwave intensity (EP) is marked using red (blue), whereas a decrease in peak intensity (EP) is shown in blue (brown). The shades of the markers show slope changes estimated using Theil-Sen's slope method, with darker shade infers larger changes, whereas lighter shade suggests small slope changes. The white shade indicates no notable slope changes.

intense irrigation operation (Guo et al., 2022; Mishra et al., 2020). For the west-central, central-northeast and coastal northeast regions, the mean timing of T_w (Figure S9a in Supporting Information S1) is clustered around the monsoon season (June-August), whereas in the hilly northeast region, humid heatwaves tend to occur in the post-monsoon period (October-December). This delayed occurrence of heatwaves is explained by the later arrival of the monsoon to the vast stretches of northeast India. The timing of $T_{w\max}$ shows a strong seasonality (Figure S9b in Supporting Information S1); more than 50% of the sites have the annual maxima humid heat clustered around the southwest monsoon season with the highest frequency in June. Overall, our findings confirm earlier assessments (Ivanovich et al., 2022; Raymond et al., 2020) that (a) humid heatwaves coincide with the southwest monsoon season, and (b) the mean timing of T_w intensity is the largest around the climatological onset time of the southwest monsoon rainfall season.

3.4. Identification of CMHP Hotspots

Figure 6 identifies the joint occurrence of CMHP events, analyzing (a) the dependence strength between drivers using the complete versus the empirical upper tail dependence measures, Kendall's τ and λ_U, (b) the lag-time between peak T_w intensity (or annual maxima $T_{w\max}$) and EP, and (c) the frequency of CMHP events. While the dependence strength considering all values shows only five stations with significant dependence, that are

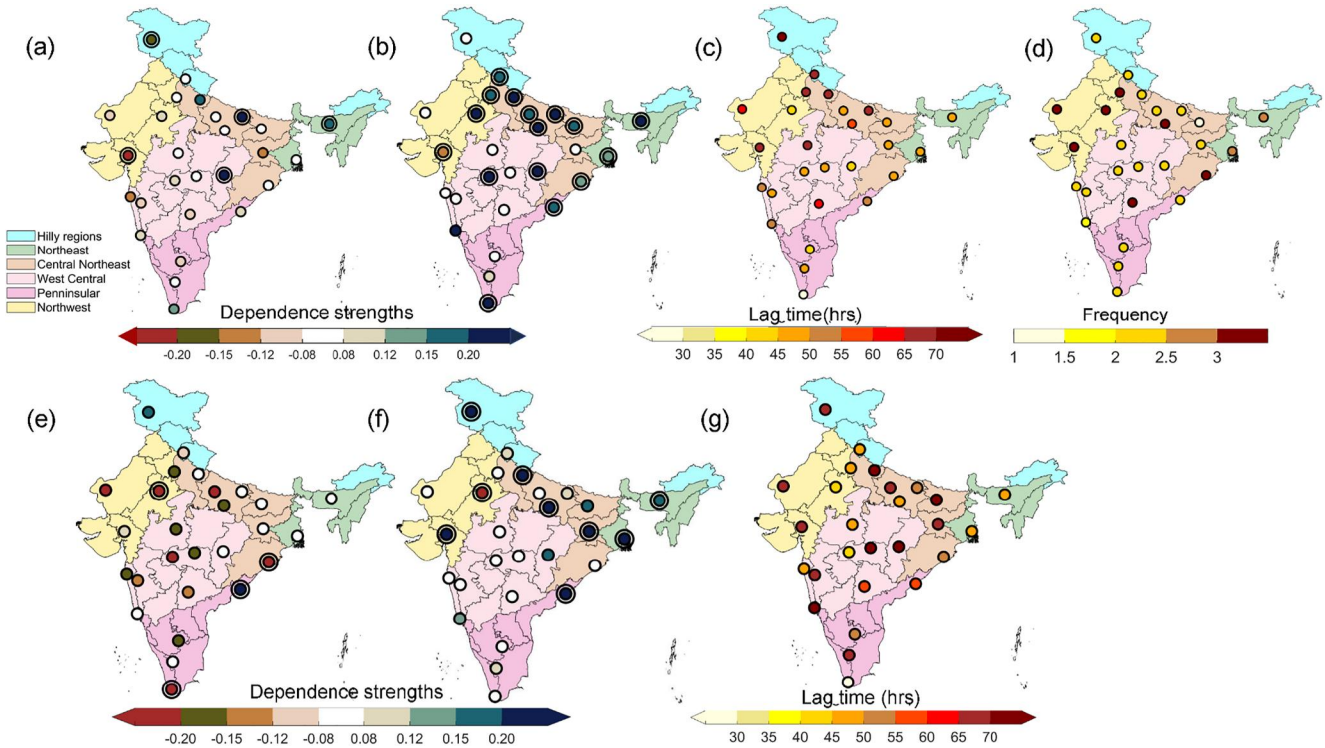

Figure 6. Spatial variations in dependence strengths, lag time and frequency of Compound Moist Heatwave-Extreme Precipitation (CMHP) events. (a) Complete dependence using Kendall's τ, and (b) tail dependence coefficient λ_U between heatwave peak intensity, T_w and the following extreme precipitation (EP) events. (c) Mean lag-time between heatwave peak and subsequent extreme rainfall peak. (d) Average (50th percentile) frequency of CMHP events per year. (e) Kendall's τ and (f) λ_U between $T_{w\max}$ and EP events. (g) Lag time between $T_{w\max}$ and subsequent EP events. Double circles indicate significant dependence (i.e., $p < 0.05$).

scattered in the north of India, the upper tail dependence is much more pronounced with a more distinct spatial pattern. Over 60% of all locations show a strong positive significant dependence. These stations with significant dependence are located, with one exception, in the northern part covering the entire IGP plain (Central-northeast), and the west-central and eastern coastal plains (Figures 6a and 6b). A similar pattern of dependence is apparent for the annual maxima $T_{w\max}$ and EP events over the IGP and eastern coastal plains (Figures 6e and 6f).

The scatterplots of lag time versus λ_U (Figures S10a and S10b in Supporting Information S1) show a smaller lag time accompanied by modest to strong correlations for gauges across the northeast regions, such as Guwahati and Kolkata (Figures 6c and 6g). The northeast regions also experience on average 2.5 CMHP events per year, indicating a stronger potential of compound events. The central northeast region shows a stronger upper-tail dependence coefficient with large counts of outlying CMHP events (Figure S10c in Supporting Information S1); however, sites in this area show a longer response time of more than 45-hr (Figures 6c and 6g). Over the northwest and western coastal plains, the complete dependence is, in general, negative. In contrast, the dependence strength at the upper tail is weaker, and in a few cases, positive across the western coastal plains. The gauges across the northwest, such as New Delhi, Jaipur, Ahmedabad, and central northeast regions, such as Prayagraj and Bhubaneshwar, experienced on average three compound events per year. Out of these gauges, except Ahmedabad where a negative λ_U is apparent, the upper-tail dependence coefficients for T_w (and $T_{w\max}$) versus EPs for other cities lies in the range of 0.14–0.23. Positive upper tail dependence coefficients imply a higher likelihood of CMHP events and, therefore, suggest hotspots of CMHP occurrence.

3.5. Seasonal Frequency of CMHP Events

The temporal evolution of CMHP frequency for each season indicates a substantial increase in the monsoon and post-monsoon seasons with trend slopes of 0.54 and 0.35 year^{-1}, respectively (Figure 7). The trends are smaller for the pre-monsoon (0.26 year^{-1}) and winter (0.18 year^{-1}) seasons. For all seasons the trends are statistically significant with a p-value <0.05 with F-test. The significant increase in seasonal trends in CMHP frequency

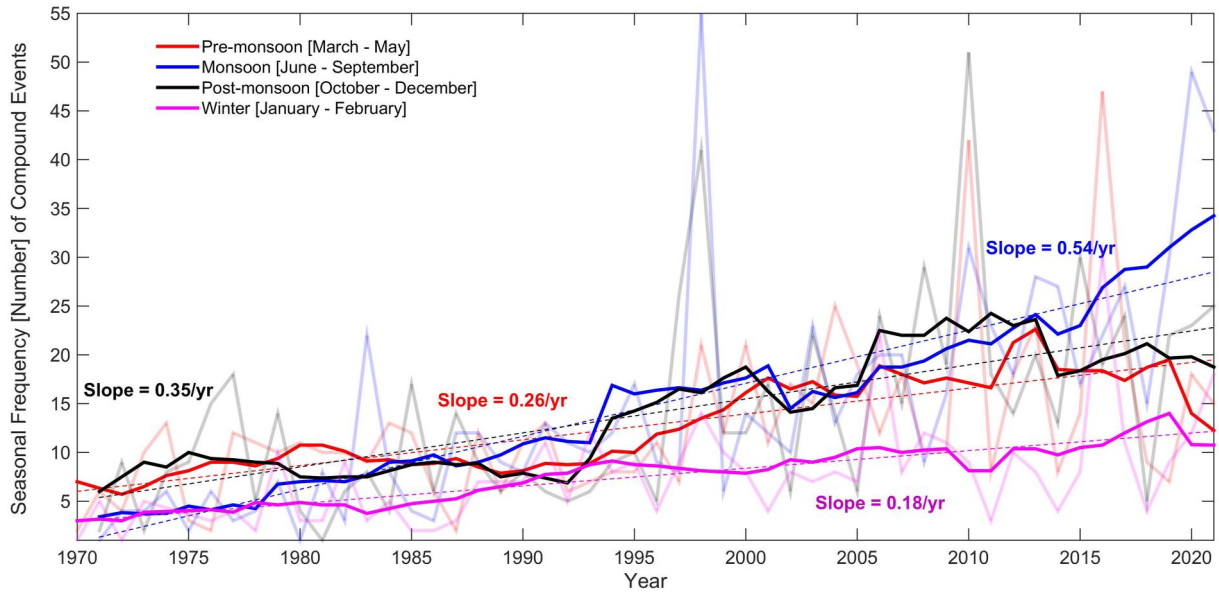

Figure 7. Seasonal frequency of Compound Moist Heatwave-Extreme Precipitation (CMHP) events. The shaded lines show the annual frequency of CMHP events for each season. The CMHP frequency is smoothed using 8-year moving average (solid lines) to emphasize the inter-annual to decadal variability in CMHP events. The changes in seasonal frequency (dashed lines) show statistically significant increasing trends for all seasons with a p-value < 0.05 with F-test.

suggests an increased risk of EPs preconditioned by humid heatwaves. The largest counts of CMHP events occurred in 2010 (with a total count of 133), followed by 1998 (131 events) considering all sites and seasons. The monsoon season of 1998 and the post-monsoon season of 2010 reported extremely high numbers of CMHP occurrences.

3.6. Changes in Conditional Exceedance Probability of Extreme Rainfall With Increasing Heatwave Duration or Return Period

We use the trivariate copula function to understand the relative changes in exceedance probability of above-average EPs for two scenarios: (a) for the 10-year humid heatwave peak intensity T_w and varying heatwave durations, d = 6, 7, 8, 9, and 10 days relative to 5-day events, (b) for the 5-day heatwave duration d and varying return periods (2, 5, 15, 20, 25, and 50-year) of heatwave peak intensities T_w relative to the 10-year event. The heat maps (Figure S11 in Supporting Information S1) presenting the relative changes in exceedance probability suggest that EP is substantially affected by both heatwave characteristics. Increasing the duration of a heatwave for the 10-year peak intensity results in lower EP values for a 67% (18/27) of sites (Figure S11a in Supporting Information S1). In contrast, increasing the heatwave amplitude for the 5-day duration results in higher EP values for ∼55% (15/27) of sites (Figure S11b in Supporting Information S1). The relative changes are more prominent if the return period of T_w increases from 2-year to 10-year. For higher return period events (≥15-year), the relative difference becomes smaller.

To understand the spatial variation, we visualize the relative changes in exceedance probability of above-average EPs for two representative extreme scenarios: (a) the 10-year heatwave peak intensity T_w with varying event durations from d = 5–10 days; (b) the 5-day heatwave duration with varying return periods of peak intensity T_w, ranging from 2-year to 50-year amplitudes (Figure 8; upper and lower panels; Tables S9 and S10 in Supporting Information S1). While for scenario (a), 33% (9 out of 27) sites show an increase in the likelihood of above-average EPs from 2% to 36%, 67% of sites show a decrease in EPs due to limited moisture availability at higher temperature associated with the longer duration of heatwave episodes (Table S9 in Supporting Information S1). In contrast, for scenario (2), ∼55% of sites show an increase in the likelihood of EPs from 3% to 31% (Table S10 in Supporting Information S1). Our findings are in agreement with earlier assessments (Ghausi et al., 2022; Robinson et al., 2021) that showed an intensification of rainfall extremes in the tropical regions, especially across the Indian subcontinent (see Figure 2 in Robinson et al., 2021) with warmer temperatures.

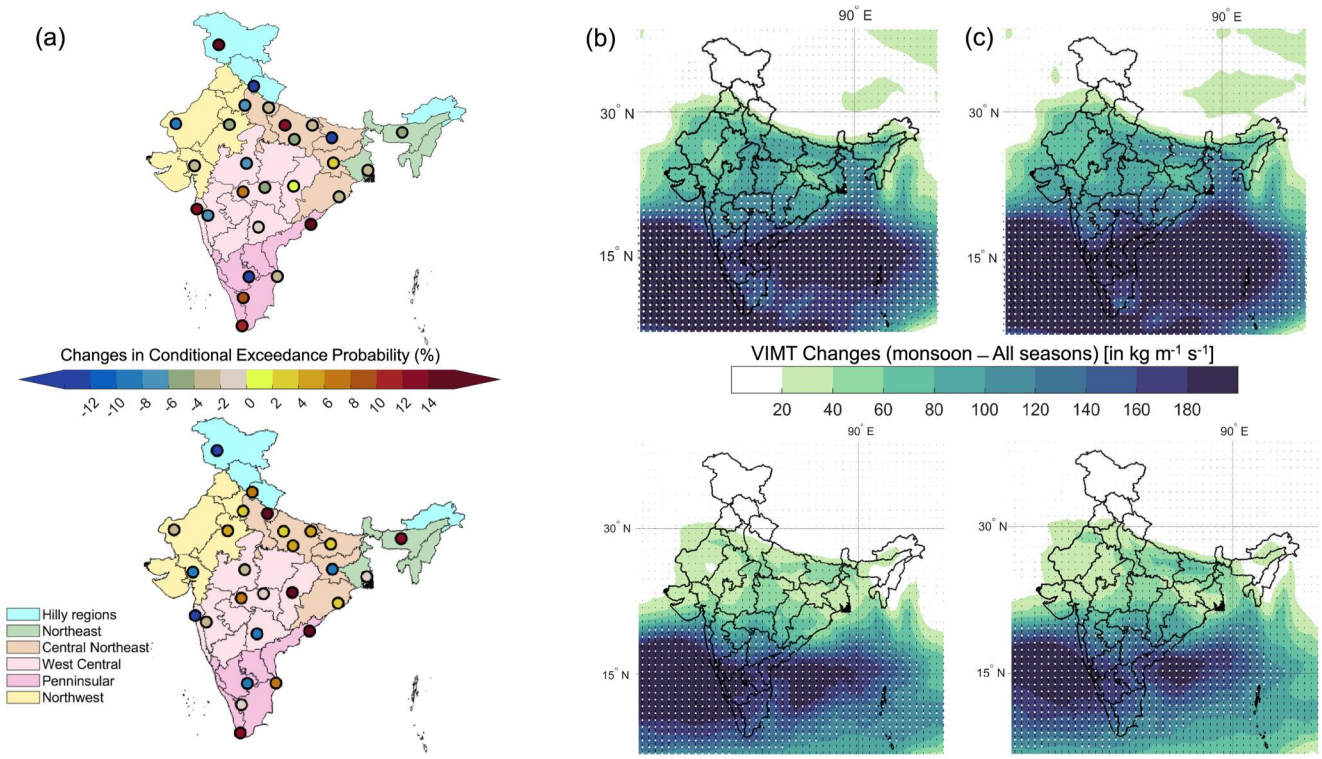

Figure 8. Changes in conditional exceedance probability of extreme precipitations (EPs) and associated drivers given (a) *top panel:* 10-year peak heatwave intensity with increasing humid heatwave duration from $d' = 5$ days to $d' = 10$ days; *bottom panel:* 5-day heatwave with increasing peak intensity from $T_w = 2$-year to $T_w = 50$-year return events. Change in mean moisture flux in the monsoon (June-September) months versus the entire year for (b) humid hot days defined by T_w (*top panel*) and $T_{w\max}$ (*bottom panel*), and for (c) days with extreme precipitation events preceded by T_w (*top panel*) and $T_{w\max}$ (*bottom panel*). Stipples in white indicate grids with vertically integrated moisture transport (VIMT) anomaly >100 kg $m^{-1}s^{-1}$ and significant at 1% significance level ($p < 0.01$). The statistical significance of VIMT anomalies are detected using the Wilcoxon rank-sum test.

Although these assessments have focused on the sensitivity of rainfall to temperature, they have not shown the impact of heatwave duration on rainfall extremes.

For scenario 1, the sites Srinagar, Lucknow, Mumbai, Visakhapatnam, and Thiruvananthapuram show a relative increase in EPs in the 12%–36% range. Out of these five cities, three cities are located in the low-elevated coastal peninsula and western coastal plain (Table S9 in Supporting Information S1). The largest increase is apparent in Srinagar (36%), situated in a hilly region with a temperate climate, followed by Visakhapatnam (31.5%) in peninsular India. In Mumbai, the above-average EP events are expected to increase from 36% to 42% (13% relative increase) for a moderate increase in heatwave duration from 5 to 10 days. On the other hand, several stations (67%, 18 out of 27) show a decline in EPs (between 1% and 16%) with increasing duration. The most significant decline is expected in Dehradun city (16%) near the Himalayan foothill, followed by Bengaluru (13%) located in the west-central region. For scenario 2, a substantial increase in above-average EPs is expected along the vast stretches of IGP, the low-elevated coasts of central northeast and southern peninsular regions. For both scenarios, Dehradun in the hilly region, Lucknow in the central northeast, Raipur and Akola in the west-central, and Visakhapatnam and Thiruvananthapuram in the peninsular region show an expected increase in above-average EPs for changing heatwave characteristics.

The maps of VIMT anomalies during the hot days (Figure 8: column b) versus the EP events (Figure 8: column c) compare the moisture transport variations during these events. The differences in daily averaged VIMT during the days of peak T_w intensity (and annual maxima $T_{w\max}$) through all seasons versus the humid hot days during monsoon months show a divergence (or decrease, shown using lighter shade in the VIMT anomaly plot) pattern, especially in the lower Gangetic Plains, and in northwest and northeast India. This indicates atmospheric blocking during humid hot days (Figure 8: column b), which corroborates findings of an earlier assessment (Dubey et al., 2021). During EP events following the peak T_w intensity (Figure 8: column c, upper panel), the moisture

convergence (or increase, shown using darker shade in the VIMT anomaly plot) strengthens cyclonic circulation over the southern region, coastal plains, pushing moisture flux towards the west-central, northeast, and central-northeast regions (Figure 8, column c: upper panel; white stipples show grids with VIMT anomaly of >100 kg m^{-1} s^{-1}, which is significant at 1% significance level). The high moisture flux from the Bay of Bengal advects towards the IGP (Figure 8, column c: upper panel shown using white stipples). During the EP events following $T_{w\max}$ (Figure 8, column c: lower panel), we find lower, however, more zonal concentration of moisture flux over the peninsula region with larger spatial coverage of positive VIMT anomalies in the range of >60–80 kg m^{-1} s^{-1} over the IGP and northeast areas (shown using darker shades). The spatial coverage of positive VIMT anomalies for the EP events following $T_{w\max}$ is, however, statistically insignificant over the IGP and northeast region, unlike the EP events following the peak T_w intensity. Taken together, the results show large changes in moisture flux over the west-central and the central northeast regions during EP days that follow humid hot days. Over the peninsular region, although VIMT anomalies show significant positive changes during the days of peak T_w intensity (and annual maxima $T_{w\max}$), the magnitude and spatial extents of significant positive VIMT anomalies are larger during the EP events (shown using darker shades). The difference in VIMT anomalies during the hot days versus EP events might be a consequence of the influence of the low-level jets, which are prominent in the monsoon-dominated areas of South Asia from June to August and are a key contributor to global moisture transport (Gimeno-Sotelo & Gimeno, 2023).

4. Discussion

4.1. Changes in Individual Drivers of CMHP Events Versus Their Nonlinear Association

The spatial distribution (Figure 5) of trends in humid heatwaves shows an increase over the northwest, west-central, and southern peninsula and a few sites in the eastern coastal plains. While intense heatwaves are caused by winds from the northwest desert that advect heat to central and northern India (Satyanarayana & Rao, 2020), intensifying irrigation practices over the IGP of the central-northeast region have further resulted in increased humid heatwave as suggested by the positive trend slopes (Figure 5). The mean timing of peak humid heatwave intensity in IGP is temporally scattered around February-August (Figures S9a and S9b in Supporting Information S1), which corroborates earlier findings of the timing of peak humid heatwave in this region, in particular, during the pre-monsoon seasons when relative humidity is low (Guo et al., 2022). The expansion of irrigated areas and the presence of atmospheric aerosols could be responsible for the increase in heat stress during the pre-monsoon period compared to the monsoon season (Figures S9a and S9b in Supporting Information S1; Guo et al., 2022; Jha et al., 2022). During the southwest monsoon season, a higher diurnal variability is observed in the eastern coastal area compared to the western coast (S. J. Reddy, 1976). Further, from June to September, north India experiences higher wet-bulb temperatures than the southern peninsula (S. J. Reddy, 1976). A recent (Dubey et al., 2021) study have shown that the "warm air intrusion" from the northwest region contribute to heat stress in the southern peninsular India (Dubey et al., 2021). As a result of the warm air intrusion, the region experiences a low-specific humidity anomaly, which prevents the entry of humid-cold air from the ocean, leading to elevated temperatures.

The trend analysis suggests a decrease in EP following the peak heatwave across several sites that are primarily concentrated around north-west, west-central and peninsular India. The rainfall in tropical regions is essentially convective in nature; however, a decline in sub-daily EP following heat stress could be due to a potential synoptic-scale linkage between cloud cover and precipitation when temperatures reach beyond 23–25°C, impacting incoming shortwave radiation, as demonstrated earlier for tropical India (Ghausi et al., 2022). An (insignificant) increase of 0.3 mm $decade^{-1}$ in EP preceded by the annual maxima $T_{w\max}$ is apparent across Dehradun in the hilly region (Figure 5d and Table S5 in Supporting Information S1), which is possibly linked to recent warming amplifications in the high-elevated regions of the Himalayas (Lutz et al., 2014; You et al., 2017). Further, the mean timing of $T_{w\max}$ for Dehradun is around June. Coincidently, Dehradun receives severe rains during the monsoon season, which is caused by eastward migrating monsoon disturbances, including cyclonic circulations, low-pressure systems or monsoon depressions that travel along the monsoon trough (A. Sharma et al., 2012). An earlier study also documented a long-term increasing trend in monsoon rainfall for Dehradun (Basistha et al., 2009).

We find that the mean lag (Figures 6c and 6g) time between peak heatwave intensity and EP events is higher for most sites located in the central northeast and hilly regions compared to sites located across the northeast and

eastern coastal plains. The lower (higher) lag times can result in a smaller (larger) frequency of CMHP occurrence per year (Figure 6d). Our results corroborate earlier studies (Devanand et al., 2019; Douglas et al., 2009; Lee et al., 2009; Sen Roy et al., 2011) that suggest intense irrigation activities over northern India have caused a weakening of early monsoon rainfall, which is responsible for a delayed shift in the timing of intense EP events over the IGP in the central northeast region, leading to a longer lag time of CMHP events. Further, the desert region of northwest India reports the highest temperature since the hot air from the Middle East enters the Indian subcontinent via this region (Satyanarayana & Rao, 2020). The dry extratropical winds associated with mid-latitude westerlies inhibit the convective instability over northwest India, which suppresses monsoon convection resulting in the weakening of monsoon rainfall (Krishnan et al., 2009). The reduced monsoon convection and weakened monsoon rainfall across the northwest region possibly explain the negative correlation between peak humid heat stress and peak rainfall over a few sites (e.g., Jaipur and Ahmedabad) of this region.

4.2. Relative Changes in Above-Average EP in Response to Heatwave Characteristics

The conditional probability model shows lower probability of extreme rainfall with increasing heatwave duration, from 5-day to 10-day, for 67% of sites. While temperature-related convection is a major driver for localized high rainfall intensities (Dowdy & Catto, 2017), lower rainfall probabilities could be due to heat-induced suppression of rainfall or moisture constraints at higher temperatures, as evident in both mean and EP over land across several regions globally (Fowler et al., 2021; Sun & Wang, 2022). Our findings corroborate with Sauter et al. (2023), who showed a modest increase in probability of rainfall preceded by heatwaves in western India as compared to the western coast. However, Sauter et al. (2023) neither considered humidity when defining heatwaves nor investigated the effect of heatwave duration on EPs. While a general agreement between our study and Sauter et al. (2023) is apparent, due to differences in definitions of heatwaves, extreme rainfall, and the sampling variability of compound events, a direct comparison between the two studies is not possible.

With an increase in peak heatwave intensity, for a given duration, >50% sites show an expected increase in short-duration rainfall extremes, confirming that an increase in humid heat exacerbates convective instability followed by precipitation extremes. Interestingly, in both scenarios, the eastern coastal plains and irrigation intensive regions show an increase in short-duration EPs. An increase in the likelihood of above-average EPs in two of the central Indian cities, Raipur and Akola, can be explained by their recent expansion in irrigation potentials in those areas (CWRD, 2023; MSDB, 2013) and the variability in the zonal moisture transport over the central Indian subcontinent (Roxy et al., 2017). Over west-central India, an increase in EP could be linked to an intensification of cyclonic vorticity generated by convective heating associated with monsoon low-pressure system (Nikumbh et al., 2020). Further, our result shows a spatially varying trend in sub-daily EPs in response to heatwave characteristics. Previous research (Ghosh et al., 2012; Paul et al., 2018) found substantial spatial heterogeneity in precipitation extremes, with opposite trends in adjoining sub-regions, which they attributed to rapid rising urbanization (Paul et al., 2018).

The sensitivity analysis (Figure 8; Figure S11a in Supporting Information S1) shows cities located within a 20 km radius of the coastline, for example, Visakhapatnam and Thiruvananthapuram in the southern peninsular coast and Mumbai in the west-central region, are expected to experience a robust rise in EPs. An expected increase in precipitation in coastal regions is due to ocean conditions driving the atmospheric circulation (Trenberth & Shea, 2005). According to a recent study (Mohanty et al., 2023), the localized EP over the Mumbai coast during monsoon seasons, when humid heatwave is likely to occur (Figure S9 in Supporting Information S1), is the result of a confluence of numerous drivers, including an abnormally high SST gradient, the orography of the Western Ghats, and a Bay of Bengal depression, which flows north-northwestward.

4.3. Implications for Further Research and for Climate Adaptation

The multiple drivers, their space-time changes and their conditional dependencies, especially at the upper tails, lead to a complex chain of causal processes of CMHP events with potentially devastating impacts (Zscheischler et al., 2018). The possible transition toward wetter or dryer patterns in response to humid heatwave characteristics poses challenges for understanding anthropogenic influences on CMHP events (Masson-Delmotte et al., 2021), operational forecasting and risk-informed decision-making (Abbaszadeh et al., 2022). Transitions to dryer/wetter rainfall patterns as consequence of increasing heat stress in a warming world may have substantial impacts on terrestrial ecosystems and built environments (Matanó et al., 2022; Yin et al., 2023). A humid heatwave that hits

ecosystems and societies may increase their vulnerability to extreme rainfall and, in turn, to flooding and associated consequences such as erosion and landslides.

As the frequency and intensity of heatwaves and EP tend to increase as a consequence of climate change (Zhou et al., 2023), and as the associated consequences for CMHP events are complex, there is a need for in-depth analyses of the interactions between heatwaves and extreme rainfall regionally, and at larger spatial scales considering multiple climate regimes in a changing climate. Over the low-latitude tropical land regions, anomalously low soil moisture often acts as a determinant of heat stress (Röthlisberger & Papritz, 2023), which potentially controls CMHP hazards. Due to the high persistency of soil moisture, this effect is deemed insignificant for variations less than a month (Dirmeyer et al., 2022), and hence not considered in our study.

Our findings underpin the role of conditioning heatwave characteristics for an expected decline or amplification in EP events. These findings suggest that expected increases in EP will have an unprecedented impact on small catchments, especially impermeable urban watersheds prone to flash floods (Faghih & Brissette, 2023). In contrast, heatwaves compounded by a decline in precipitation impact vegetation productivity and depletion of soil moisture reserves, which gradually evolve into the development of dryer state, escalating the likelihood of persistent droughts (Ganguli, 2023; Mukherjee et al., 2023).

5. Conclusions

This paper investigates the statistical coupling between heatwave characteristics and following short-duration precipitation extremes. A positive (negative) coupling between interdependent drivers translates into a larger (lower) risk of sequential compound heat stress-extreme precipitation events. For this, we introduce a copula-based conditional probability framework that defines a conditional joint probability in which humid heatwave characteristics, namely heatwave intensity and duration, determine the conditional probability of sub-daily extreme rainfall. Using this framework, we compare the impact of conditional duration and peak amplitude distributions on short-duration precipitation extremes and derive associated uncertainty (PDF). We find that with a modest increase in heatwave characteristics (i.e., either duration or peak heatwave intensity) during hot-humid days, large amplifications in short-duration EP events are apparent over the coastal cities compared to cities in the IGP. An expected amplification in short-duration EPs in response to climate warming and corresponding heatwave attributes suggests susceptibility to cascade hazards, that is, heat stress - moderate to severe rain-induced flooding in coastal areas. This is alarming since the recovery period tends to shorten when multiple CMHP events occur in quick succession, overtaxing disaster management capabilities. However, it should be noted that we do not evaluate the flooding related damages.

Our proof-of-concept approach may be adapted to any geographic region to locate "hotspots" of CMHP events using observations and climate model output. Insights from the study will benefit risk management, flash flood forecasting, and the (re)insurance industry, especially over the Indian subcontinent, which is prone to heat stress. As climate shocks increase, we may expect enhanced humid heat stress-short-duration EP coupling with a shift in the seasonal timing of such events, which has profound social and economic consequences (Buermann et al., 2013; Marelle et al., 2018). To fully understand the complex feedback mechanisms that govern the climate system and develop resilient adaptation strategies to such extremes, future evaluations are required to unveil the effects of anthropogenic forcing on CMHP extremes.

Data Availability Statement

Hydrometeorological records are obtained from the IMD, Pune—Data Supply Portal (https://cdsp.imdpune.gov.in/home_dsp.php and https://dsp.imdpune.gov.in/data_supply_service.php#procedure). The population data is obtained from the Census India website for the Census year 2011, namely from files "C-14 City: Population In Five Year Age-Group By Residence And Sex-2011", "A-04: Towns and urban agglomerations classified by population size class in 2011 with variation between 1901 and 2011—Class I (population of 100,000 and above)", and "A-04: Towns and urban agglomerations classified by population size class in 2011 with variation between 1901 and 2011—Class II (population of 50,000 to 99,999)," available freely at Census of India website in the webpage Census tables https://censusindia.gov.in/census.website/data/census-tables. The VIMT time series are downloaded from the European Centre for Medium-Range Weather Forecasts (ECMWF)'s ERA-Interim product archived at: https://www.ecmwf.int/en/forecasts/dataset/ecmwf-reanalysis-interim.

Acknowledgments
The work received funding from the Women Involvement in Science and Engineering Research (WISER) project of Indo-German Science and Technology Centre (IGSTC) with funding ID: IGSTC/WISER 2022/PG/47/2022-23/514. P.G. acknowledge Pritam Goraksh Daundkar's (a Master's student supervised by P.G. at IIT-KGP) contribution to meteorological data collection from the IMD.

References

Abbaszadeh, P., Muñoz, D. F., Moftakhari, H., Jafarzadegan, K., & Moradkhani, H. (2022). Perspective on uncertainty quantification and reduction in compound flood modeling and forecasting. *iScience*, *25*(10), 105201. https://doi.org/10.1016/j.isci.2022.105201

AghaKouchak, A., Sellars, S., & Sorooshian, S. (2013). Methods of tail dependence estimation. In A. AghaKouchak, D. Easterling, K. Hsu, S. Schubert, & S. Sorooshian (Eds.), *Extremes in a changing climate* (Vol. 65, pp. 163–179). Springer.

Ali, H., Fowler, H. J., Lenderink, G., Lewis, E., & Pritchard, D. (2021). Consistent large-scale response of hourly extreme precipitation to temperature variation over land. *Geophysical Research Letters*, *48*(4), e2020GL090317. https://doi.org/10.1029/2020GL090317

Bansal, A., Cherbuin, N., Davis, D. L., Peek, M. J., Wingett, A., Christensen, B. K., et al. (2023). Heatwaves and wildfires suffocate our healthy start to life: Time to assess impact and take action. *The Lancet Planetary Health*, *7*(8), e718–e725. https://doi.org/10.1016/s2542-5196(23)00134-1

Barton, Y., Giannakaki, P., Waldow, H., von Chevalier, C., Pfahl, S., & Martius, O. (2016). Clustering of regional-scale extreme precipitation events in southern Switzerland. *Monthly Weather Review*, *144*(1), 347–369. https://doi.org/10.1175/MWR-D-15-0205.1

Basistha, A., Arya, D. S., & Goel, N. K. (2009). Analysis of historical changes in rainfall in the Indian Himalayas. *International Journal of Climatology: A Journal of the Royal Meteorological Society*, *29*(4), 555–572. https://doi.org/10.1002/joc.1706

Beillard, M. J., & Singh, S. K. (2022). *Extreme temperatures Scorch Indian wheat production (No. IN2022-0045), report number: IN2022-0045*. United States Department of Agriculture (USDA) Foreign Agricultural Service. Retrieved from https://apps.fas.usda.gov

Bose, M. (2023). Increasing heat stress to trigger extreme weather across India, crop damage. Retrieved from https://www.deccanherald.com/science-and-environment/increasing-heat-stress-to-trigger-extreme-weather-across-india-crop-damage-1200646.html

Buermann, W., Bikash, P. R., Jung, M., Burn, D. H., & Reichstein, M. (2013). Earlier springs decrease peak summer productivity in North American boreal forests. *Environmental Research Letters*, *8*(2), 024027. https://doi.org/10.1088/1748-9326/8/2/024027

Bui, A., Johnson, F., & Wasko, C. (2019). The relationship of atmospheric air temperature and dew point temperature to extreme rainfall. *Environmental Research Letters*, *14*(7), 074025. https://doi.org/10.1088/1748-9326/ab2a26

Burnham, K. P., & Anderson, D. R. (2003). *Model selection and multimodel inference: A practical information-theoretic approach*. Springer Science & Business Media.

Ceccherini, G., Russo, S., Ameztoy, I., Marchese, A. F., & Carmona-Moreno, C. (2017). Heat waves in Africa 1981–2015, observations and reanalysis. *Natural Hazards and Earth System Sciences*, *17*(1), 115–125. https://doi.org/10.5194/nhess-17-115-2017

Chauhan, C. (2023). Warmer than normal temperature in west, north India. Retrieved from https://www.hindustantimes.com/india-news/warmer-than-normal-temperature-in-west-north-india-101676661436446.html

CWRD (Chhattisgarh Water Resources Department). (2023). Irrigation potential of Chattisgarh. Retrieved from https://cgwrd.in/organisation/activities/irrigation-potential.html

Davis, R. E., McGregor, G. R., & Enfield, K. B. (2016). Humidity: A review and primer on atmospheric moisture and human health. *Environmental Research*, *144*, 106–116. https://doi.org/10.1016/j.envres.2015.10.014

De Leo, F., Besio, G., Briganti, R., & Vanem, E. (2021). Non-stationary extreme value analysis of sea states based on linear trends. Analysis of annual maxima series of significant wave height and peak period in the Mediterranean Sea. *Coastal Engineering*, *167*, 103896. https://doi.org/10.1016/j.coastaleng.2021.103896

Devanand, A., Huang, M., Ashfaq, M., Barik, B., & Ghosh, S. (2019). Choice of irrigation water management practice affects Indian summer monsoon rainfall and its extremes. *Geophysical Research Letters*, *46*(15), 9126–9135. https://doi.org/10.1029/2019GL083875

Dirmeyer, P. A., Sridhar Mantripragada, R. S., Gay, B. A., & Klein, D. K. D. (2022). Evolution of land surface feedbacks on extreme heat: Adapting existing coupling metrics to a changing climate. *Frontiers in Environmental Science*, *10*, 1650. https://doi.org/10.3389/fenvs.2022.949250

Domeisen, D. I., Eltahir, E. A., Fischer, E. M., Knutti, R., Perkins-Kirkpatrick, S. E., Schär, C., et al. (2022). Prediction and projection of heatwaves. *Nature Reviews Earth & Environment*, *4*, 1–15. https://doi.org/10.1038/s43017-022-00371-z

Douglas, E. M., Beltrán-Przekurat, A., Niyogi, D., Pielke, R. A., & Vörösmarty, C. J. (2009). The impact of agricultural intensification and irrigation on land–atmosphere interactions and Indian monsoon precipitation—A mesoscale modeling perspective. *Global and Planetary Change*, *67*(1), 117–128. https://doi.org/10.1016/j.gloplacha.2008.12.007

Dowdy, A. J., & Catto, J. L. (2017). Extreme weather caused by concurrent cyclone, front and thunderstorm occurrences. *Scientific Reports*, *7*(1), 40359. https://doi.org/10.1038/srep40359

Dubey, A. K., Kumar, P., Saharwardi, M. S., & Javed, A. (2021). Understanding the hot season dynamics and variability across India. *Weather and Climate Extremes*, *32*, 100317. https://doi.org/10.1016/j.wace.2021.100317

EM-DAT, E.-D. (2023). EM-DAT: The international disaster database. Retrieved from https://www.emdat.be/

Faghih, M., & Brissette, F. (2023). Temporal and spatial amplification of extreme rainfall and extreme floods in a warmer climate. *Journal of Hydrometeorology*, *1*(8), 1331–1347. https://doi.org/10.1175/JHM-D-22-0224.1

Fan, Y., Li, Y., Bejan, A., Wang, Y., & Yang, X. (2017). Horizontal extent of the urban heat dome flow. *Scientific Reports*, *7*(1), 1–10. https://doi.org/10.1038/s41598-017-09917-4

FAO (Food and Agriculture Organization of the United Nations). (2022). GIEWS country brief on India. Retrieved from https://www.fao.org/giews/countrybrief/country.jsp?code=IND&lang=ar

Feng, K., Ouyang, M., & Lin, N. (2022). Tropical cyclone-blackout-heatwave compound hazard resilience in a changing climate. *Nature Communications*, *13*(1), 4421. https://doi.org/10.1038/s41467-022-32018-4

Fischer, E., & Knutti, R. (2016). Observed heavy precipitation increase confirms theory and early models. *Nature Climate Change*, *6*(11), 986–991. https://doi.org/10.1038/nclimate3110

Fowler, H. J., Lenderink, G., Prein, A. F., Westra, S., Allan, R. P., Ban, N., et al. (2021). Anthropogenic intensification of short-duration rainfall extremes. *Nature Reviews Earth & Environment*, *2*(2), 107–122. https://doi.org/10.1038/s43017-020-00128-6

Frahm, G., Junker, M., & Schmidt, R. (2005). Estimating the tail-dependence coefficient: Properties and pitfalls. *Insurance: Mathematics and Economics*, *37*(1), 80–100. https://doi.org/10.1016/j.insmatheco.2005.05.008

Ganguli, P. (2023). Amplified risk of compound heat stress-dry spells in Urban India. *Climate Dynamics*, *60*(3–4), 1061–1078. https://doi.org/10.1007/s00382-022-06324-y

Genest, C., Ghoudi, K., & Rivest, L.-P. (1995). A semiparametric estimation procedure of dependence parameters in multivariate families of distributions. *Biometrika*, *82*(3), 543–552. https://doi.org/10.1093/biomet/82.3.543

Genest, C., Rémillard, B., & Beaudoin, D. (2009). Goodness-of-fit tests for copulas: A review and a power study. *Insurance: Mathematics and Economics*, *44*(2), 199–213. https://doi.org/10.1016/j.insmatheco.2007.10.005

Ghausi, S. A., Ghosh, S., & Kleidon, A. (2022). Breakdown in precipitation–temperature scaling over India predominantly explained by cloud-driven cooling. *Hydrology and Earth System Sciences*, *26*(16), 4431–4446. https://doi.org/10.5194/hess-26-4431-2022

Ghosh, S., Das, D., Kao, S.-C., & Ganguly, A. R. (2012). Lack of uniform trends but increasing spatial variability in observed Indian rainfall extremes. *Nature Climate Change*, *2*(2), 86–91. https://doi.org/10.1038/nclimate1327

Gimeno-Sotelo, L., & Gimeno, L. (2023). Where does the link between atmospheric moisture transport and extreme precipitation matter? *Weather and Climate Extremes*, *39*, 100536. https://doi.org/10.1016/j.wace.2022.100536

Gori, A., Lin, N., & Xi, D. (2020). Tropical cyclone compound flood hazard assessment: From investigating drivers to quantifying extreme water levels. *Earth's Future*, *8*(12), e2020EF001660. https://doi.org/10.1029/2020EF001660

GSDMA (Gujarat State Disaster Management Authority). (2023). Heat wave action plan: 2022–23. Vadodara. Retrieved from https://vmc.gov.in/pdf/Annoucement/2022/Heat%20wave%20action%20plan%202022-23.pdf

Guntu, R. K., Merz, B., & Agarwal, A. (2023). Increased likelihood of compound dry and hot extremes in India. *Atmospheric Research*, *290*, 106789. https://doi.org/10.1016/j.atmosres.2023.106789

Guo, Q., Zhou, X., Satoh, Y., & Oki, T. (2022). Irrigated cropland expansion exacerbates the urban moist heat stress in northern India. *Environmental Research Letters*, *17*(5), 054013. https://doi.org/10.1088/1748-9326/ac64b6

Ha, K.-J., Seo, Y.-W., Yeo, J.-H., Timmermann, A., Chung, E.-S., Franzke, C. L., et al. (2022). Dynamics and characteristics of dry and moist heatwaves over East Asia. *Npj Climate and Atmospheric Science*, *5*(1), 49. https://doi.org/10.1038/s41612-022-00272-4

Hassler, B., & Lauer, A. (2021). Comparison of reanalysis and observational precipitation datasets including ERA5 and WFDE5. *Atmosphere*, *12*(11), 1462. https://doi.org/10.3390/atmos12111462

Held, I. M., & Soden, B. J. (2006). Robust responses of the hydrological cycle to global warming. *Journal of Climate*, *19*(21), 5686–5699. https://doi.org/10.1175/JCLI3990.1

Hindustan Times. (2022). UN agency WMO, IMD sound alarm on heatwaves; experts say must document deaths. Retrieved from https://www.hindustantimes.com/india-news/wmo-and-imd-sound-alarm-on-heatwaves-experts-say-must-document-deaths-101651261074523.html

Hino, M., & Burke, M. (2021). The effect of information about climate risk on property values. *Proceedings of the National Academy of Sciences*, *118*(17), e2003374118. https://doi.org/10.1073/pnas.2003374118

Ilampooranan, I., Van Meter, K. J., & Basu, N. B. (2019). A race against time: Modeling time lags in watershed response. *Water Resources Research*, *55*(5), 3941–3959. https://doi.org/10.1029/2018wr023815

Im, E.-S., Pal, J. S., & Eltahir, E. A. (2017). Deadly heat waves projected in the densely populated agricultural regions of South Asia. *Science Advances*, *3*(8), e1603322. https://doi.org/10.1126/sciadv.1603322

IMD (India Meteorological Department). (2022). *Statement on climate of India during 2022* (pp. 1–11). Ministry of Earth Sciences, Government of India.

Ivanovich, C., Anderson, W., Horton, R., Raymond, C., & Sobel, A. (2022). The influence of intraseasonal oscillations on humid heat in the Persian Gulf and South Asia. *Journal of Climate*, *35*(13), 4309–4329. https://doi.org/10.1175/JCLI-D-21-0488.1

Jha, R., Mondal, A., Devanand, A., Roxy, M. K., & Ghosh, S. (2022). Limited influence of irrigation on pre-monsoon heat stress in the Indo-Gangetic Plain. *Nature Communications*, *13*(1), 4275. https://doi.org/10.1038/s41467-022-31962-5

Keellings, D., & Moradkhani, H. (2020). Spatiotemporal evolution of heat wave severity and coverage across the United States. *Geophysical Research Letters*, *47*(9), e2020GL087097. https://doi.org/10.1029/2020GL087097

Kemter, M., Merz, B., Marwan, N., Vorogushyn, S., & Blöschl, G. (2020). Joint trends in flood magnitudes and spatial extents across Europe. *Geophysical Research Letters*, *47*(7), e2020GL087464. https://doi.org/10.1029/2020GL087464

Kotz, M., Levermann, A., & Wenz, L. (2022). The effect of rainfall changes on economic production. *Nature*, *601*(7892), 223–227. https://doi.org/10.1038/s41586-021-04283-8

Krishnan, R., Kumar, V., Sugi, M., & Yoshimura, J. (2009). Internal feedbacks from monsoon–midlatitude interactions during droughts in the Indian summer monsoon. *Journal of the Atmospheric Sciences*, *66*(3), 553–578. https://doi.org/10.1175/2008jas2723.1

Kruczkiewicz, A., Klopp, J., Fisher, J., Mason, S., McClain, S., Sheekh, N. M., et al. (2021). Compound risks and complex emergencies require new approaches to preparedness. *Proceedings of the National Academy of Sciences*, *118*(19), e2106795118. https://doi.org/10.1073/pnas.2106795118

Leach, N. J., Weisheimer, A., Allen, M. R., & Palmer, T. (2021). Forecast-based attribution of a winter heatwave within the limit of predictability. *Proceedings of the National Academy of Sciences*, *118*(49), e2112087118. https://doi.org/10.1073/pnas.2112087118

Lee, E., Chase, T. N., Rajagopalan, B., Barry, R. G., Biggs, T. W., & Lawrence, P. J. (2009). Effects of irrigation and vegetation activity on early Indian summer monsoon variability. *International Journal of Climatology*, *29*(4), 573–581. https://doi.org/10.1002/joc.1721

Lélé, M. I., Leslie, L. M., & Lamb, P. J. (2015). Analysis of low-level atmospheric moisture transport associated with the West African monsoon. *Journal of Climate*, *28*(11), 4414–4430. https://doi.org/10.1175/jcli-d-14-00746.1

Lenton, T. M., Xu, C., Abrams, J. F., Ghadiali, A., Loriani, S., Sakschewski, B., et al. (2023). Quantifying the human cost of global warming. *Nature Sustainability*, *6*(10), 1–11. https://doi.org/10.1038/s41893-023-01132-6

Li, C., Gu, X., Slater, L. J., Liu, J., Li, J., Zhang, X., & Kong, D. (2023). Urbanization-induced increases in heavy precipitation are magnified by moist heatwaves in an urban agglomeration of East China. *Journal of Climate*, *36*(2), 693–709. https://doi.org/10.1175/JCLI-D-22-0223.1

Li, Y., Fowler, H. J., Argüeso, D., Blenkinsop, S., Evans, J. P., Lenderink, G., et al. (2020). Strong intensification of hourly rainfall extremes by urbanization. *Geophysical Research Letters*, *47*(14), e2020GL088758. https://doi.org/10.1029/2020GL088758

Liu, J., & Niyogi, D. (2019). Meta-analysis of urbanization impact on rainfall modification. *Scientific Reports*, *9*(1), 7301. https://doi.org/10.1038/s41598-019-42494-2

Lobell, D. B., Sibley, A., & Ivan Ortiz-Monasterio, J. (2012). Extreme heat effects on wheat senescence in India. *Nature Climate Change*, *2*(3), 186–189. https://doi.org/10.1038/nclimate1356

Loughran, T. F., Perkins-Kirkpatrick, S. E., & Alexander, L. V. (2017). Understanding the spatio-temporal influence of climate variability on Australian heatwaves. *International Journal of Climatology*, *37*(10), 3963–3975. https://doi.org/10.1002/joc.4971

Lutz, A. F., Immerzeel, W. W., Shrestha, A. B., & Bierkens, M. F. P. (2014). Consistent increase in High Asia's runoff due to increasing glacier melt and precipitation. *Nature Climate Change*, *4*(7), 587–592. https://doi.org/10.1038/nclimate2237

Lyddon, C., Robins, P., Lewis, M., Barkwith, A., Vasilopoulos, G., Haigh, I., & Coulthard, T. (2023). Historic spatial patterns of storm-driven compound events in UK estuaries. *Estuaries and Coasts*, *46*(1), 30–56. https://doi.org/10.1007/s12237-022-01115-4

Maharana, P., & Dimri, A. P. (2014). Study of seasonal climatology and interannual variability over India and its subregions using a regional climate model (RegCM3). *Journal of Earth System Science*, *123*(5), 1147–1169. https://doi.org/10.1007/s12040-014-0447-7

Marelle, L., Myhre, G., Hodnebrog, Ø., Sillmann, J., & Samset, B. H. (2018). The changing seasonality of extreme daily precipitation. *Geophysical Research Letters*, *45*(20), 11–352. https://doi.org/10.1029/2018gl079567

Masson-Delmotte, V., Zhai, P., Pirani, A., Connors, S. L., Péan, C., Berger, S., et al. (2021). Climate change 2021: The physical science basis. In *Contribution of working group I to the sixth assessment report of the intergovernmental panel on climate change* (Vol. 2).

Matanó, A., de Ruiter, M. C., Koehler, J., Ward, P. J., & Van Loon, A. F. (2022). Caught between extremes: Understanding human-water interactions during drought-to-flood events in the Horn of Africa. *Earth's Future*, *10*(9), e2022EF002747. https://doi.org/10.1029/2022ef002747

Matthews, T., Wilby, R. L., & Murphy, C. (2019). An emerging tropical cyclone–deadly heat compound hazard. *Nature Climate Change*, *9*(8), 602–606. https://doi.org/10.1038/s41558-019-0525-6

Mazdiyasni, O., Sadegh, M., Chiang, F., & AghaKouchak, A. (2019). Heat wave intensity duration frequency curve: A multivariate approach for hazard and attribution analysis. *Scientific Reports*, *9*(1), 14117. https://doi.org/10.1038/s41598-019-50643-w

Miralles, D. G., Gentine, P., Seneviratne, S. I., & Teuling, A. J. (2019). Land–atmospheric feedbacks during droughts and heatwaves: State of the science and current challenges. *Annals of the New York Academy of Sciences*, *1436*(1), 19–35. https://doi.org/10.1111/nyas.13912

Mishra, V., Ambika, A. K., Asoka, A., Aadhar, S., Buzan, J., Kumar, R., & Huber, M. (2020). Moist heat stress extremes in India enhanced by irrigation. *Nature Geoscience*, *13*(11), 722–728. https://doi.org/10.1038/s41561-020-00650-8

Moccia, B., Mineo, C., Ridolfi, E., Russo, F., & Napolitano, F. (2021). Probability distributions of daily rainfall extremes in Lazio and Sicily, Italy, and design rainfall inferences. *Journal of Hydrology: Regional Studies*, *33*, 100771. https://doi.org/10.1016/j.ejrh.2020.100771

Mohan, V. (2023). India feels the heat: Hottest February recorded since 1901. Retrieved from http://timesofindia.indiatimes.com/articleshow/98320212.cms?from=mdr%20Check%20for%20Jaisalmer&utm_source=contentofinterest&utm_medium=text&utm_campaign=cppst

Mohanty, S., Swain, M., Nadimpalli, R., Osuri, K. K., Mohanty, U. C., Patel, P., & Niyogi, D. (2023). Meteorological conditions of extreme heavy rains over coastal city Mumbai. *Journal of Applied Meteorology and Climatology*, *62*(2), 191–208. https://doi.org/10.1175/jamc-d-21-0223.1

MSDB (Maharashtra State Data Bank). (2013). Irrigation and flood control. Report no. DSA 5/17. Retrieved from https://mahasdb.maharashtra.gov.in/SDB_Reports/Akola/PDF/2010-11_Akola_DSA_5_17.pdf

Mukherjee, S., Mishra, A. K., Zscheischler, J., & Entekhabi, D. (2023). Interaction between dry and hot extremes at a global scale using a cascade modeling framework. *Nature Communications*, *14*(1), 277. https://doi.org/10.1038/s41467-022-35748-7

Nageswararao, M. M., Sinha, P., Mohanty, U. C., & Mishra, S. (2020). Occurrence of more heat waves over the central East coast of India in the recent warming Era. *Pure and Applied Geophysics*, *177*(2), 1143–1155. https://doi.org/10.1007/s00024-019-02304-2

Nelsen, R. B. (2013). *An introduction to copulas* (Vol. 139). Springer.

Nikumbh, A. C., Chakraborty, A., Bhat, G. S., & Frierson, D. M. W. (2020). Large-scale extreme rainfall-producing synoptic systems of the Indian summer monsoon. *Geophysical Research Letters*, *47*(11), e2020GL088403. https://doi.org/10.1029/2020GL088403

Ning, G., Luo, M., Zhang, W., Liu, Z., Wang, S., & Gao, T. (2022). Rising risks of compound extreme heat-precipitation events in China. *International Journal of Climatology*, *42*(11), 5785–5795. https://doi.org/10.1002/joc.7561

Nogueira, M. (2020). Inter-comparison of ERA-5, ERA-interim and GPCP rainfall over the last 40 years: Process-based analysis of systematic and random differences. *Journal of Hydrology*, *583*, 124632. https://doi.org/10.1016/j.jhydrol.2020.124632

ORGCC (Office of the Registrar General & Census Commissioner, India). (2022). India—A-04 (I): Towns and urban agglomerations classified by population size class in 2011 with variation between 1901 and 2011—Class I (population of 100,000 and above). Retrieved from https://censusindia.gov.in/nada/index.php/catalog/42876

Ortiz, L. E., Gonzalez, J. E., Wu, W., Schoonen, M., Tongue, J., & Bornstein, R. (2018). New York city impacts on a regional heat wave. *Journal of Applied Meteorology and Climatology*, *57*(4), 837–851. https://doi.org/10.1175/jamc-d-17-0125.1

Paul, S., Ghosh, S., Mathew, M., Devanand, A., Karmakar, S., & Niyogi, D. (2018). Increased spatial variability and intensification of extreme monsoon rainfall due to urbanization. *Scientific Reports*, *8*(1), 3918. https://doi.org/10.1038/s41598-018-22322-9

Perkins, S. E. (2015). A review on the scientific understanding of heatwaves—Their measurement, driving mechanisms, and changes at the global scale. *Atmospheric Research*, *164*, 242–267. https://doi.org/10.1016/j.atmosres.2015.05.014

Prein, A. F., Rasmussen, R. M., Ikeda, K., Liu, C., Clark, M. P., & Holland, G. J. (2017). The future intensification of hourly precipitation extremes. *Nature Climate Change*, *7*(1), 48–52. https://doi.org/10.1038/nclimate3168

Qin, J., Liu, H., & Li, B. (2023). Unprecedented warming in northwestern India during April of 2022: Roles of local forcing and atmospheric Rossby wave. *Geoscience Letters*, *10*(1), 2. https://doi.org/10.1186/s40562-022-00257-4

Raghavendra, A., Dai, A., Milrad, S. M., & Cloutier-Bisbee, S. R. (2019). Floridian heatwaves and extreme precipitation: Future climate projections. *Climate Dynamics*, *52*(1), 495–508. https://doi.org/10.1007/s00382-018-4148-9

Rajeev, A., Mahto, S. S., & Mishra, V. (2022). Climate warming and summer monsoon breaks drive compound dry and hot extremes in India. *iScience*, *25*(11), 105377. https://doi.org/10.1016/j.isci.2022.105377

Rajeev, A., & Mishra, V. (2022). Observational evidence of increasing compound tropical cyclone-moist heat extremes in India. *Earth's Future*, *10*(12), e2022EF002992. https://doi.org/10.1029/2022EF002992

Rajeevan, M., Bhate, J., & Jaswal, A. K. (2008). Analysis of variability and trends of extreme rainfall events over India using 104 years of gridded daily rainfall data. *Geophysical Research Letters*, *35*(18), L18707. https://doi.org/10.1029/2008GL035143

Ratnam, J. V., Behera, S. K., Ratna, S. B., Rajeevan, M., & Yamagata, T. (2016). Anatomy of Indian heatwaves. *Scientific Reports*, *6*(1), 1–11. https://doi.org/10.1038/srep24395

Raymond, C., Matthews, T., & Horton, R. M. (2020). The emergence of heat and humidity too severe for human tolerance. *Science Advances*, *6*(19), eaaw1838. https://doi.org/10.1126/sciadv.aaw1838

Reddy, M. J., & Ganguli, P. (2013). Spatio-temporal analysis and derivation of copula-based intensity–area–frequency curves for droughts in western Rajasthan (India). *Stochastic Environmental Research and Risk Assessment*, *27*(8), 1975–1989. https://doi.org/10.1007/s00477-013-0732-z

Reddy, S. J. (1976). Wet bulb temperature distribution over India. *Mausam*, *27*(2), 167–172. https://doi.org/10.54302/mausam.v27i2.2432

Robinson, A., Lehmann, J., Barriopedro, D., Rahmstorf, S., & Coumou, D. (2021). Increasing heat and rainfall extremes now far outside the historical climate. *Npj Climate and Atmospheric Science*, *4*(1), 45. https://doi.org/10.1038/s41612-021-00202-w

Roderick, T. P., Wasko, C., & Sharma, A. (2019). Atmospheric moisture measurements explain increases in tropical rainfall extremes. *Geophysical Research Letters*, *46*(3), 1375–1382. https://doi.org/10.1029/2018gl080833

Röthlisberger, M., & Papritz, L. (2023). Quantifying the physical processes leading to atmospheric hot extremes at a global scale. *Nature Geoscience*, *16*(3), 210–216. https://doi.org/10.1038/s41561-023-01126-1

Roxy, M. K., Ghosh, S., Pathak, A., Athulya, R., Mujumdar, M., Murtugudde, R., et al. (2017). A threefold rise in widespread extreme rain events over central India. *Nature Communications*, *8*(1), 708. https://doi.org/10.1038/s41467-017-00744-9

Salvadori, G., Tomasicchio, G. R., & D'Alessandro, F. (2014). Practical guidelines for multivariate analysis and design in coastal and off-shore engineering. *Coastal Engineering*, *88*, 1–14. https://doi.org/10.1016/j.coastaleng.2014.01.011

Satyanarayana, G. C. H., & Rao, D. B. (2020). Phenology of heat waves over India. *Atmospheric Research*, *245*, 105078. https://doi.org/10.1016/j.atmosres.2020.105078

Sauter, C., Fowler, H. J., Westra, S., Ali, H., Peleg, N., & White, C. J. (2023). Compound extreme hourly rainfall preconditioned by heatwaves most likely in the mid-latitudes. *Weather and Climate Extremes*, *40*, 100563. https://doi.org/10.1016/j.wace.2023.100563

Sen, P. K. (1968). Estimates of the regression coefficient based on Kendall's tau. *Journal of the American Statistical Association*, *63*(324), 1379–1389. https://doi.org/10.1080/01621459.1968.10480934

Seneviratne, S., Zhang, X., Adnan, M., Badi, W., Dereczynski, C., Di Lu, A., et al. (2021). Chapter 11: Weather and climate extreme events in a changing climate. In V. Masson-Delmotte, P. Zhai, A. Pirani, S. L. Connors, C. Péan, S. Berger, et al. (Eds.), *Climate change 2021: The physical science basis. Contribution of working group I to the sixth assessment report of the intergovernmental panel on climate change* (pp. 1513–1766). Cambridge University Press. https://doi.org/10.1017/9781009157896.013

Sen Roy, S., Mahmood, R., Quintanar, A. I., & Gonzalez, A. (2011). Impacts of irrigation on dry season precipitation in India. *Theoretical and Applied Climatology*, *104*(1), 193–207. https://doi.org/10.1007/s00704-010-0338-z

Serinaldi, F., Bárdossy, A., & Kilsby, C. G. (2015). Upper tail dependence in rainfall extremes: Would we know it if we saw it? *Stochastic Environmental Research and Risk Assessment*, *29*(4), 1211–1233. https://doi.org/10.1007/s00477-014-0946-8

Sharma, A., Singh, O. P., & Saklani, M. M. (2012). *Climate of Dehradun* (pp. 1–77). India Meteorological Department. Retrieved from https://amssdelhi.gov.in/news_events/Dehradun_Climate.pdf

Sharma, S., & Mujumdar, P. (2017). Increasing frequency and spatial extent of concurrent meteorological droughts and heatwaves in India. *Scientific Reports*, *7*(1), 15582. https://doi.org/10.1038/s41598-017-15896-3

Simpkins, G. (2023). Compound tropical cyclone–heatwaves on the rise. *Nature Reviews Earth & Environment*, *4*(1), 3-3. https://doi.org/10.1038/s43017-022-00386-6

Singh, C., & Kumar, S. V. J. (2018). Meteorological conditions for development of heat wave over Coastal Andhra Pradesh and Telangana. *The Journal of Indian Geophysical Union*, *3*, 349–358.

Stone, B., Jr., Mallen, E., Rajput, M., Gronlund, C. J., Broadbent, A. M., Krayenhoff, E. S., et al. (2021). Compound climate and infrastructure events: How electrical grid failure alters heat wave risk. *Environmental Science & Technology*, *55*(10), 6957–6964. https://doi.org/10.1021/acs.est.1c00024

Sun, X., & Wang, G. (2022). Causes for the negative scaling of extreme precipitation at high temperatures. *Journal of Climate*, *35*(18), 6119–6134. https://doi.org/10.1175/jcli-d-22-0142.1

Trenberth, K. E. (1999). Atmospheric moisture recycling: Role of advection and local evaporation. *Journal of Climate*, *12*(5), 1368–1381. https://doi.org/10.1175/1520-0442(1999)012<1368:amrroa>2.0.co;2

Trenberth, K. E., & Shea, D. J. (2005). Relationships between precipitation and surface temperature. *Geophysical Research Letters*, *32*(14), L14703. https://doi.org/10.1029/2005GL022760

Tuholske, C., Caylor, K., Funk, C., Verdin, A., Sweeney, S., Grace, K., et al. (2021). Global urban population exposure to extreme heat. *Proceedings of the National Academy of Sciences*, *118*(41), e2024792118. https://doi.org/10.1073/pnas.2024792118

van Zomeren, J., & van Delden, A. (2007). Vertically integrated moisture flux convergence as a predictor of thunderstorms. *Atmospheric Research*, *83*(2–4), 435–445. https://doi.org/10.1016/j.atmosres.2005.08.015

Vo, T. T., Hu, L., Xue, L., Li, Q., & Chen, S. (2023). Urban effects on local cloud patterns. *Proceedings of the National Academy of Sciences*, *120*(21), e2216765120. https://doi.org/10.1073/pnas.2216765120

Wang, P., Yang, Y., Xue, D., Qu, Y., Tang, J., Leung, L. R., & Liao, H. (2023). Increasing compound hazards of tropical cyclones and heatwaves over southeastern coast of China under climate warming. *Journal of Climate*, *36*(7), 2243–2257. https://doi.org/10.1175/jcli-d-22-0279.1

Wang, S. S.-Y., Kim, H., Coumou, D., Yoon, J.-H., Zhao, L., & Gillies, R. R. (2019). Consecutive extreme flooding and heat wave in Japan: Are they becoming a norm? *Atmospheric Science Letters*, *20*(10), e933. https://doi.org/10.1002/asl.933

Wehner, M., Stone, D., Krishnan, H., AchutaRao, K., & Castillo, F. (2016). The deadly combination of heat and humidity in India and Pakistan in summer 2015. *Bulletin of the American Meteorological Society*, *97*(12), S81–S86. https://doi.org/10.1175/bams-d-16-0145.1

Wehrli, K., Luo, F., Hauser, M., Shiogama, H., Tokuda, D., Kim, H., et al. (2022). The ExtremeX global climate model experiment: Investigating thermodynamic and dynamic processes contributing to weather and climate extremes. *Earth System Dynamics*, *13*(3), 1167–1196. https://doi.org/10.5194/esd-13-1167-2022

Willett, K. M., Gillett, N. P., Jones, P. D., & Thorne, P. W. (2007). Attribution of observed surface humidity changes to human influence. *Nature*, *449*(7163), 710–712. https://doi.org/10.1038/nature06207

WMO. (2023). Heat and health. Retrieved from https://www.who.int/news-room/fact-sheets/detail/climate-change-heat-and-health

Yang, J., Zhao, L., & Oleson, K. (2023). Large humidity effects on urban heat exposure and cooling 1086 challenges under climate change. *Environmental Research Letters*, *18*(4), 044024. https://doi.org/10.1088/1748-9326/acc475ss

Yang, X., Zeng, G., Zhang, G., Li, J., Li, Z., & Hao, Z. (2021). Interdecadal variations of different types of summer heat waves in Northeast China associated with AMO and PDO. *Journal of Climate*, *34*(19), 7783–7797. https://doi.org/10.1175/jcli-d-20-0939.1

Ye, H., & Fetzer, E. J. (2019). Asymmetrical shift toward longer dry spells associated with warming temperatures during Russian summers. *Geophysical Research Letters*, *46*(20), 11455–11462. https://doi.org/10.1029/2019gl084748

Ye, H., Fetzer, E. J., Behrangi, A., Wong, S., Lambrigtsen, B. H., Wang, C. Y., et al. (2016). Increasing daily precipitation intensity associated with warmer air temperatures over northern Eurasia. *Journal of Climate*, *29*(2), 623–636. https://doi.org/10.1175/jcli-d-14-00771.1

Yin, J., Gentine, P., Slater, L., Gu, L., Pokhrel, Y., Hanasaki, N., et al. (2023). Future socio-ecosystem productivity threatened by compound drought–heatwave events. *Nature Sustainability*, *6*(3), 1–14. https://doi.org/10.1038/s41893-022-01024-1

Yin, J., Slater, L., Gu, L., Liao, Z., Guo, S., & Gentine, P. (2022). Global increases in lethal compound heat stress: Hydrological drought hazards under climate change. *Geophysical Research Letters*, *49*(18), e2022GL100880. https://doi.org/10.1029/2022GL100880

You, J., & Wang, S. (2021). Higher probability of occurrence of Hotter and shorter heat waves followed by heavy rainfall. *Geophysical Research Letters*, *48*(17), e2021GL094831. https://doi.org/10.1029/2021GL094831

You, J., Wang, S., Zhang, B., Raymond, C., & Matthews, T. (2023). Growing threats from swings between hot and wet extremes in a warmer world. *Geophysical Research Letters*, *50*(14), e2023GL104075. https://doi.org/10.1029/2023GL104075

You, Q.-L., Ren, G.-Y., Zhang, Y.-Q., Ren, Y.-Y., Sun, X.-B., Zhan, Y.-J., et al. (2017). An overview of studies of observed climate change in the Hindu Kush Himalayan (HKH) region. *Advances in Climate Change Research*, *8*(3), 141–147. https://doi.org/10.1016/j.accre.2017.04.001

Zhang, K., Cao, C., Chu, H., Zhao, L., Zhao, J., & Lee, X. (2023). Increased heat risk in wet climate induced by urban humid heat. *Nature*, *617*(7962), 1–5. https://doi.org/10.1038/s41586-023-05911-1

Zhang, L., & Singh, V. P. (2019). *Copulas and their applications in water Resources engineering*. Cambridge University Press.

Zhang, W., & Villarini, G. (2020). Deadly compound heat stress-flooding hazard across the Central United States. *Geophysical Research Letters*, *47*(15), e2020GL089185. https://doi.org/10.1029/2020GL089185

Zhang, Y., & Boos, W. R. (2021). Risk of intense precipitation accompanying extreme wet-bulb temperatures. In *AGU fall meeting 2021, paper ID: GC51C-03*. AGU.

Zhou, S., Yu, B., & Zhang, Y. (2023). Global concurrent climate extremes exacerbated by anthropogenic climate change. *Science Advances*, *9*(10), eabo1638. https://doi.org/10.1126/sciadv.abo1638

Zscheischler, J., Martius, O., Westra, S., Bevacqua, E., Raymond, C., Horton, R. M., et al. (2020). A typology of compound weather and climate events. *Nature Reviews Earth & Environment*, *1*(7), 333–347. https://doi.org/10.1038/s43017-020-0060-z

Zscheischler, J., Westra, S., Van Den Hurk, B. J., Seneviratne, S. I., Ward, P. J., Pitman, A., et al. (2018). Future climate risk from compound events. *Nature Climate Change*, *8*(6), 469–477. https://doi.org/10.1038/s41558-018-0156-3

References From the Supporting Information

Burnham, K. P., & Anderson, D. R. (2004). Multimodel inference: Understanding AIC and BIC in model selection. *Sociological Methods & Research*, *33*(2), 261–304. https://doi.org/10.1177/0049124104268644

Cheng, L., & AghaKouchak, A. (2014). Nonstationary precipitation intensity-duration-frequency curves for infrastructure design in a changing climate. *Scientific Reports*, *4*(1), srep07093. https://doi.org/10.1038/srep07093

Ivanovich, C., Horton, R. M., & Sobel, A. H. (2021). Extreme humid heat during South Asian summer monsoon breaks. In *AGU fall meeting 2021*. AGU.

Katz, R. W. (2013). Statistical methods for nonstationary extremes. In A. AghaKouchak, D. Easterling, K. Hsu, S. Schubert, & S. Sorooshian (Eds.), *Extremes in a changing climate: Detection, analysis and uncertainty* (pp. 15–37). Springer.

Li, D., & Bou-Zeid, E. (2013). Synergistic interactions between urban heat islands and heat waves: The impact in cities is larger than the sum of its parts. *Journal of Applied Meteorology and Climatology*, *52*(9), 2051–2064. https://doi.org/10.1175/jamc-d-13-02.1

Renard, B., Sun, X., & Lang, M. (2013). Bayesian methods for non-stationary extreme value analysis. In *Extremes in a changing climate* (pp. 39–95). Springer.

Poulin, A., Huard, D., Favre, A.-C., & Pugin, S. (2007). Importance of tail dependence in bivariate frequency analysis. *Journal of Hydrologic Engineering*, *12*(4), 394–403. https://doi.org/10.1061/(asce)1084-0699(2007)12:4(394)